A New Approach to Identifying the Real Effects of Uncertainty Shocks

Minchul Shin
University of Illinois

Molin Zhong*
Federal Reserve Board

This version: May, 2016

Abstract

This paper proposes a multivariate stochastic volatility-in-vector autoregression model called the conditional autoregressive inverse Wishart-in-VAR (CAIW-in-VAR) model as a framework for studying the real effects of uncertainty shocks. We make three contributions to the literature. First, the uncertainty shocks we analyze are estimated directly from macroeconomic data so they are associated with changes in the volatility of the shocks hitting the macroeconomy. Second, we advance a new approach to identify uncertainty shocks by placing limited economic restrictions on the first and second moment responses to these shocks. Third, we consider an extension of the sign restrictions methodology of Uhlig (2005) to uncertainty shocks. To illustrate our methods, we ask what is the role of financial markets in transmitting uncertainty shocks to the real economy? We find evidence that an increase in uncertainty leads to a decline in industrial production only if associated with a deterioration in financial conditions.

Key words: Uncertainty, vector autoregression, volatility-in-mean, Wishart process, multivariate stochastic volatility.

JEL codes: C11, C32, E32

*Correspondence: Minchul Shin: 214 David Kinley Hall, 1407 W. Gregory, Urbana, Illinois 61801. E-mail: mincshin@illinois.edu. Molin Zhong: 20th Street and Constitution Avenue N.W., Washington, D.C. 20551. E-mail: molin.zhong@frb.gov. We are grateful for the advice of our advisors Frank Diebold, Jesús Fernández-Villaverde, and Frank Schorfheide. We also thank David Arseneau, Dario Caldara, Thorsten Drautzburg, Bora Durdu, Rochelle Edge, Luca Guerrieri, Pablo Guerrón-Quintana, Mohammad Jahan-Parvar, Jihyung Lee, Christian Matthes, Michael McCracken, Juan Rubio-Ramírez, Chiara Scotti, Shu Wu, Tao Zha, Ross Askanazi, Jacob Warren, as well as seminar participants at the Federal Reserve Bank of Kansas City, University of Illinois, University of Kansas, Penn Econometrics reading group, Federal Reserve Board, Midwest Econometrics Group 2015, Midwest Macro Meetings 2015, SNDE 2016 for useful comments. The views expressed in this paper are solely the responsibility of the authors and should not be interpreted as reflecting the views of the Board of Governors of the Federal Reserve System or of any other person associated with the Federal Reserve System.

1 Introduction

What are the real effects of uncertainty on the macroeconomy? This question has been challenging to analyze empirically because uncertainty is not observed. To tackle this empirical problem, the literature has proposed a variety of different approaches. One dominant approach popularized by Bloom (2009) is to include an uncertainty proxy variable, such as the VIX, into an otherwise standard vector autoregression. In theory, this proxy variable is meant to capture uncertainty, but usually we do not know exactly what this variable measures. This issue becomes even more complicated if we believe that there may be multiple types of uncertainty shocks that each affect the agents' decisions in different ways. For example, one may expect that uncertainty arising from real activity could affect the economy differently from uncertainty originating in the financial markets. Insofar as the uncertainty proxy truly measures uncertainty, it would confound the different types of uncertainty shocks into one overall shock that is difficult to interpret. Another approach taken in the literature is to write down a full-blown structural model (e.g. DSGE model or structural VAR) and attach stochastic volatilities to the identified structural shocks. In this way, one can study multiple uncertainty shocks. A potentially large cost, however, is the need to identify the entire structure of the economy before estimation. These identifying restrictions may severely distort the empirical results.

In this paper, we propose a new strategy to identify the real effects of uncertainty shocks that seeks to simultaneously address both empirical issues. We begin by introducing a vector autoregressive model with multivariate stochastic volatility that allows for the volatility-in-mean effect. We then show how to impose restrictions on the mean and volatility responses of observed economic variables to an uncertainty shock of interest. These response restrictions could come from a priori theorizing and shape the class of uncertainty shocks the researcher is investigating. This methodology can handle sign restrictions on either the mean or volatility responses and is well suited when the researcher wants to identify a subset of uncertainty shocks without imposing further modeling assumptions.

Our new strategy for identifying the real effects of uncertainty shocks connects with our multivariate stochastic volatility process called the conditional autoregressive inverse Wishart volatility model[1]. The structure of the volatility dynamics makes it such that the process can be written in a linear vector autoregressive form with innovations that are martingale

[1]This volatility process, introduced into the financial econometrics literature by Golosnoy et al. (2012) and in macroeconomics by Karapanagiotidis (2012), models time-varying volatility with the Wishart family of distributions (See Philipov and Glickman, 2006; Gourieroux et al., 2009; Fox and West, 2013, for alternative autoregressive Wishart models.).

difference sequences. Upon writing the volatility process in vector autoregressive form, it is possible to impose restrictions directly on the responses to the volatility shocks without having to consider any explicit restrictions on the first moment shocks. We emphasize, however, that our identification methodology does not require any specific volatility process and is in fact amenable to many different reduced-form processes. We use the conditional autoregressive inverse Wishart volatility process for its flexibility and attractive property that its estimation results do not depend on the ordering of the observable variables in the system.

Our approach has three main novelties relative to the current literature. First, we have an econometric model allowing for time-varying second moments, so we estimate uncertainty directly from the macroeconomic data. This is unlike the literature that uses proxies such as the VIX, Economic Policy Uncertainty Index, or forecast disagreement to identify uncertainty shocks[2] (Bloom, 2009; Leduc and Liu, 2012; Baker et al., 2013; Scotti, 2013; Bachmann et al., 2013) and is closer to the approach taken in Jurado et al. (2015). One criticism of the volatility proxy approach is that it is unclear what the proxies truly capture[3]. With our approach, we do not run into this interpretation issue. Relative to Jurado et al. (2015), who first extract common fluctuations in stochastic volatility from a large panel of macroeconomic and financial variables and then run a VAR on macroeconomic variables, we have a one-step estimation procedure and identify different sources of uncertainty shocks through economic restrictions.

Second, the form of our volatility process allows us to put economic restrictions directly on the responses to the uncertainty shocks of interest. Specifically, we can place restrictions on the expected responses of the first moments and second moments to uncertainty shocks. Previous approaches in the literature to investigate the real effects of uncertainty shocks with a stochastic volatility-in-vector autoregression model, such as Mumtaz and Zanetti (2013), Creal and Wu (2014), Jo (2014), and Montes-Galdon (2015), initially identify first moment structural shocks and then put stochastic volatility on those shocks. Our complementary approach is arguably more appropriate when the researcher would like to restrict the uncertainty shock under consideration through its first and second moment responses and does not want to risk further misspecification. Importantly, the researcher can be explicit about the conditions imposed without fully identifying the entire set of first and second moment

[2]There are ample papers in this category. The interested reader is referred to Bloom (2014) and papers cited in that paper.

[3]For instance, it is unclear whether VIX measures macroeconomic uncertainty or just uncertainty in the financial sector. Moreover, these approaches do not allow the volatility proxies to change the forecast error variance of economic variables in the VAR system, which might not be consistent with the role of uncertainty in the economy.

Third, we consider an extension of the sign restrictions approach of Uhlig (2005) to uncertainty shocks. Sign restrictions allow the researcher to impose directional responses on a set of first and second moments to uncertainty shocks at various horizons while remaining agnostic about the responses outside of the set. The previous literature on the real effects of uncertainty shocks has not considered this identification strategy[4]. An example of a first moment restriction is that an uncertainty shock transmitted through the financial sector worsens a financial conditions indicator in expectation for a certain horizon. An example of a second moment restriction is that an uncertainty shock increases the conditional variance of the innovations to all variables in the economy in expectation for a certain horizon.

As an illustration of our empirical framework, we investigate the relationship between the financial market and uncertainty shocks. We estimate a $4-$variable version of our model on monthly data with industrial production, the consumer price index, the federal funds rate, and the excess bond premium (EBP) of Gilchrist and Zakrajsek (2012). We use two different strategies to identify the real effects of an uncertainty shock. In the first case, we impose only that uncertainty increases in the economy, which is a contemporaneous second moment sign restriction that the conditional variances of all shocks hitting the economy increase. There is some evidence of a decline in industrial production following an uncertainty shock, but the response is not significant. Crucially, there does not seem to be any significant change in financial conditions following the uncertainty shock. In our second exercise, we further impose a multi-step first moment sign restriction that financial conditions worsen in expectation for 3 months after the uncertainty shock. This additional restriction leads to the uncertainty shock producing a significant decline in industrial production for 15 months. The response is hump-shaped with a maximal posterior median decline of around -0.15% following a 1 standard deviation uncertainty shock. These results complement the findings

[4]Many important extensions are made after Uhlig (2005)'s paper. Among others, Rubio-Ramirez et al. (2010) study global identification and develop a number of efficient algorithms. Arias et al. (2014) further extend the algorithm so that one can properly and efficiently generate draws from an agnostic prior (the uniform distribution with respect to the Haar measure on the set of orthogonal matrices) conditional on some linear restrictions. Baumeister and Hamilton (2015) discuss an unintended consequence of the use of this agnostic Haar prior. Our paper is different from these because we focus on the identification of shocks to the second moments, which these papers do not discuss. We focus on the pure-sign restriction identification approach using the agnostic Haar prior.

There are also papers that utilize the sign restriction identification strategy to study the real effect of uncertainty shocks in conjunction with volatility proxies (Ferreira, 2014). However, the sign restriction approach is not studied in the context of a VAR model with time-varying volatility. On the other hand, Baumeister and Peersman (2013) adopt the sign restriction methodology within the time-varying Bayesian VAR framework. They do not consider the real effects of uncertainty shocks, which is the main point of our paper.

of Caldara et al. (2016) and Ferreira (2014), who find that the financial channel is important in transmitting uncertainty shocks.

We give theoretical grounding to our imposed sign restrictions using a calibrated version of the Gertler and Karadi (2011) model. We discuss model-produced responses from two sources of volatility shocks: capital quality volatility, which we interpret as financial sector uncertainty, and permanent TFP volatility, which we interpret as real activity uncertainty. Both volatility shocks lead to an increase in volatility in the observable variables, consistent with our second moment restriction. A capital quality volatility shock produces impulse response functions consistent with our imposed first moment restriction as well. Higher capital quality uncertainty increases the riskiness of capital, which decreases the incentive to invest and the price of capital, leading to an increase in spreads. Moreover, the increased uncertainty combined with the tightening of financial conditions leads to a decline in output, consistent with our empirical results. On the other hand, a permanent TFP volatility shock does not satisfy the first moment restriction. The precautionary savings channel generated by higher TFP uncertainty increases the attractiveness of investment, which then leads to an increase in the price of capital and a decrease in spreads. Therefore, we interpret our responses as likely being driven by fluctuations in uncertainty in the financial sector, in line with recent results by Ludvigson et al. (2015). This divergence of responses in spreads is important because it shows that a reasonably calibrated dynamic equilibrium model produces different comovements in observables following different uncertainty shocks.

Our work speaks to three main literatures. First, we contribute to the empirical literature investigating the real effects of uncertainty shocks. One strand of the literature, as mentioned already, uses identified innovations to volatility proxies in vector autoregressions to identify macroeconomic movements from uncertainty shocks. The second strand of literature, also previously addressed, uses the stochastic volatility-in-vector autoregression model to analyze the real effects of uncertainty shocks. The third strand of literature, exemplified by Fernandez-Villaverde et al. (2011), Leduc and Liu (2012), Born and Pfeifer (2014), Basu and Bundick (2015), Fernandez-Villaverde et al. (2015), and Schorfheide et al. (2016) uses a fully structural dynamic equilibrium model to investigate these effects. One strategy is to first estimate the stochastic volatility from a vector autoregression and then feed the extracted process into a dynamic equilibrium model. Another strategy is to match impulse response functions from uncertainty shocks in a dynamic equilibrium model to the same responses from a proxy VAR regression. Relative to this work, we propose a new model that can investigate the real effects of uncertainty shocks while potentially limiting misspecification concerns via imposing limited economic restrictions. We also consider sign restriction identification of uncertainty shocks. We hope this model will become a useful tool to guide

researchers in determining the important sources of the real effects of uncertainty in the economy.

The second literature with which we connect is the work on conditional heteroskedasticity-in-mean. This work begins with the ARCH-in-mean model proposed in Engle et al. (1987). Other important work using the model includes Domowitz and Hakkio (1985), which investigates the existence of a risk premium in the foreign exchange market. French et al. (1987) first propose the GARCH-in-mean model in the financial economics context. Elder (2004), for inflation uncertainty, and Elder and Serletis (2010), for oil price uncertainty, use the model to investigate the volatility-in-mean effect in macroeconomic applications. Working with a stochastic volatility-in-mean model allows us to consider impulse responses to volatility shocks with no movements in the level innovations, which corresponds more closely to the notion of an uncertainty shock. Because GARCH-in-mean models do not have an independent source of variation driving volatility, they have a more cumbersome time producing these impulse responses. Koopman and Uspensky (2002) propose the univariate stochastic volatility-in-mean model. To answer many of our questions, a multivariate extension to the model is required, which we provide.

Indeed, there are papers that develop and study the stochastic volatility-in-mean effect in a multivariate framework. One approach imposes restrictions on the level structural shocks to indirectly identify the uncertainty shocks (Mumtaz and Zanetti, 2013; Creal and Wu, 2014; Jo, 2014; Montes-Galdon, 2015; Mumtaz and Theodoridis, 2016). In this paper, we propose a novel identification strategy for the real effects of uncertainty shocks by imposing economic restrictions directly on the uncertainty shock impulse response functions. A second approach assumes a common factor structure in the volatility fluctuations of individual macroeconomic series. It is possible to study the volatility-in-mean effect by first estimating this common factor outside of a VAR system (Jurado et al. (2015)), treat it as a volatility proxy, and then put it into the VAR ex post. Recently, Carriero et al. (2016) provide important methodological advancements by developing a joint estimation approach where extraction of the common volatility factor and estimation of the volatility-in-mean effect are done simultaneously in a large VAR system. Our approach jointly estimates the volatility and other VAR parameters as well; however, we do not assume a common volatility structure and try to give individual volatility shocks an economic meaning.

Finally, our modeling framework builds off of a line of research modeling vector autoregressions with time-varying volatility, beginning with Uhlig (1997). Other important contributions in this field include Cogley and Sargent (2005), Primiceri (2005), and Sims and Zha (2006). These papers are concerned with whether stochastic volatility, representing

changes in the nature of shocks hitting the economy, or coefficient changes, representing shifts in the underlying relationships in the economy, are more responsible for the evolving nature of macroeconomic movements in the U.S. We also consider a vector autoregression with stochastic volatility, but we allow the stochastic volatility to have a conditional mean effect as well. Therefore, while our model builds off of this literature, the questions we aim to answer are quite different. In principle, we can allow for coefficient drift in conjunction with the volatility-in-mean effect, as in Mumtaz and Theodoridis (2016), but for clarity of presentation, we shut off that channel.

The plan of the paper is as follows. In section 2, we present the model and discuss our framework for analyzing the real effects of uncertainty shocks. In section 3, we introduce our Markov chain Monte Carlo sampler and our algorithms to compute impulse responses. Section 4 contains our empirical application on the financial sector and uncertainty shocks and section 5 concludes.

2 Model

In this section, we lay out our proposed conditional autoregressive inverse Wishart-in-vector autoregression (CAIW-in-VAR) model. We begin by discussing our model specification. We then provide details on our volatility process and discuss the advantages of our modeling strategy. Finally, we introduce our novel identification strategy for the real effects of uncertainty shocks. We note that our framework is especially amenable to the circumstances where the researcher would like to impose only limited economic restrictions.

2.1 Model specification

We consider the following vector autoregression with multivariate stochastic volatility,

$$Y_t = \mu + \Phi Y_{t-1} + Bf(\Sigma_t) + \epsilon_t, \quad \epsilon_t|\Sigma_t \sim N(0,\ \Sigma_t) \tag{1}$$

where Y_t and μ are $k \times 1$ vectors, Φ is a $k \times k$ matrix, B is a $k \times l$ matrix (or vector), and $f(\cdot)$ is a known function that maps a $k \times k$ matrix into an $l \times 1$ vector. The forecast error ϵ_t is conditionally multivariate normal with a $k \times k$ time-varying covariance matrix Σ_t.

The term $Bf(\Sigma_t)$ captures the phenomenon called the "real effect of uncertainty shock" in macroeconomics, which allows fluctuations in the volatility of the shocks to change the conditional mean of the process. In a structural model with optimizing agents, this effect

would come from agents' optimal responses to changes in risk in the economy. In our paper, we present an econometric model that can allow for these effects.

The specification of the function $f(\Sigma_t)$ is left up to the researcher as long as $f(\Sigma_t)$ enters in the conditional mean equation linearly through B[5]. In our empirical application, we specify the function $f(\Sigma_t)$ as the logarithm of the diagonal elements of Σ_t. We prefer this specification for the $f(\Sigma_t)$ function because it mimics the way fluctuations in uncertainty impact the first moments in a third-order perturbed dynamic equilibrium model.

Volatility process. We model the multivariate stochastic volatility with Wishart processes as in Philipov and Glickman (2006), Golosnoy et al. (2012), and Karapanagiotidis (2012),

$$\Sigma_t|\nu, S_{t-1} \sim IW(\nu, S_{t-1}^{-1}), \tag{2}$$

where $\nu > k+1$ is a scalar. The dynamics of the multivariate stochastic volatility are modeled by a $k \times k$ matrix S_t, which is defined with two additional parameter matrices C and A.

$$S_t = \frac{1}{(\nu-k-1)}(C + A\Sigma_t A')^{-1} \tag{3}$$

C is a $k \times k$ positive definite matrix that governs the long-run mean of the multivariate volatility process. A is a $k \times k$ matrix that governs the dynamic properties of the volatility matrix process. ν is a degrees of freedom parameter that governs the conditional variance of the Σ_t random variable. This formulation ensures that the resulting scale matrix S_t is symmetric and positive definite.

Note that the process is formulated in a way that the conditional mean of the volatility matrix has the following simple form

$$E[\Sigma_t|\mathcal{F}_{t-1}] = C + A\Sigma_{t-1}A' \tag{4}$$

and

$$Cov(\Sigma_{ij,t},\ \Sigma_{lm,t}|\mathcal{F}_{t-1}) = \frac{2\Psi_{ij,t}\Psi_{lm,t} + (\nu-k+1)(\Psi_{il,t}\Psi_{jm,t} + \Psi_{im,t}\Psi_{lj,t})}{(\nu-k)(\nu-k-3)} \tag{5}$$

where $\mathcal{F}_{t-1} = \{\Sigma_{t-1}, \Sigma_{t-2}, ...\}$ and $\Psi_t = C + A\Sigma_{t-1}A'$. This delivers a convenient linear representation for the multivariate volatility process with innovations that are martingale difference sequences,

$$\sigma_t = \overline{C} + \overline{A}\sigma_{t-1} + \overline{v}_t, \quad E[\overline{v}_t|\mathcal{F}_{t-1}] = 0 \quad \text{and} \quad E[\overline{v}_t\overline{v}_s'|\mathcal{F}_{t-1}] = 0, \quad \forall s \neq t \tag{6}$$

[5]We list a few specifications for $f(\Sigma_t)$: $\log(diag(\Sigma_t)), diag(chol(\Sigma_t)), diag(\Sigma_t)$, and $vech(\Sigma_t)$.

where $\sigma_t = vech(\Sigma_t)$, $\overline{C} = vech(C)$ and

$$\overline{A} = L_n(A \otimes A)D_n$$

where $vec(x) = D_n vech(x)$ and $vech(x) = L_n vec(x)$.

This formulation of the volatility model allows us to clearly pinpoint the time t shock to volatility, $\overline{v}_t$, which we call the uncertainty shock. We focus our identifying restrictions on this shock.

In addition, the VAR form of the volatility process proves key to deriving unconditional moments and giving stationarity conditions, as discussed in Golosnoy et al. (2012).

2.2 Identification of uncertainty shocks

Our primary goal in this paper is to identify the effects of uncertainty shocks. Once we obtain the posterior distribution of unknown parameters in the CAIW-in-VAR model, we can analyze the impact of shocks ($\overline{v}_t$) that move uncertainty Σ_t. Identifying uncertainty shocks brings along the usual challenges of identification present in the structural VAR literature. It is difficult to interpret impulse response functions and variance decompositions in terms of $\overline{v}_t$ shocks because they are contemporaneously correlated with each other. That is, an increase in one of the elements in $\overline{v}_t$ from equation 6 (e.g., the volatility of the innovation to real activity) is potentially due to different sources (e.g., either uncertainty originating in the real economy or the financial markets). In this section, we discuss how we can distinguish various sources of fluctuations in the economic variables' forecast error variances and covariances. We call these fluctuations changes in uncertainty. Our discussion in this section is based on fixed parameters. We postpone a discussion of the estimation and computation method for the unknown parameters in the CAIW-in-VAR model in section 3.

Given the linear representation of the volatility process, we can focus our attention on equation 6. We write the time t uncertainty shock ($\overline{v}_t$) as a linear function of uncorrelated unit-variance shocks ($\overline{v}_t^*$), so we have

$$\overline{v}_t = R_t \overline{v}_t^* \quad \text{or} \quad R_t^{-1}\overline{v}_t = \overline{v}_t^*, \tag{7}$$

where R_t is a $k \times k$ invertible matrix. The conditional variance-covariance matrix of $\overline{v}_t^*$ is an identity matrix, $Var(\overline{v}_t^* | \mathcal{F}_{t-1}) = I_k$. We impose restrictions on the impulse response functions to the uncertainty shocks $\overline{v}_t^*$. Note that there is an important difference between

our uncertainty shocks and structural first moment shocks (ϵ_t^*) identified from the reduced-form level shocks (ϵ_t), which have the following relationship

$$\epsilon_t = H_t \epsilon_t^* \quad \text{or} \quad H_t^{-1}\epsilon_t = \epsilon_t^*,$$

where H_t is a $k \times k$ invertible matrix. Unlike structural level shocks (ϵ_t^*), our uncertainty shocks ($\overline{v}_t^*$) have a contemporaneous impact on both the stochastic covariance matrix (Σ_t) as well as the conditional mean of the observed variables (Y_t).

It turns out that within the CAIW-in-VAR model framework, we can still utilize identification methods presented in the structural VAR literature. This possibility has not been recognized so far in the literature and we view this as an advantage of our modeling framework. To see this, recall the VAR representation of the CAIW process,

$$\sigma_t = \overline{C} + \overline{A}\sigma_{t-1} + \overline{v}_t, \quad E[\overline{v}_t|\mathcal{F}_{t-1}] = 0 \quad \text{and} \quad E[\overline{v}_t\overline{v}_s'|\mathcal{F}_{t-1}] = 0, \, \forall s \neq t, \quad E[\overline{v}_t\overline{v}_t'|\mathcal{F}_{t-1}] = \Omega_t$$

where Ω_t is the conditional variance of σ_t given the information set at time $t-1$ and is a closed-form function of Σ_{t-1}. The VAR framework naturally allows us to use the identification strategies developed in the structural VAR literature to identify uncertainty shocks. It allows us to put identifying restrictions directly on the uncertainty shocks. In this manner, we can focus on identifying uncertainty shocks, which are the objects we are interested in. In this paper, we focus on the sign restrictions approach.

Another advantage of our model is that we can identify a subset of uncertainty shocks. To see this, first note that the identification of an uncertainty shock is to choose a matrix R_t that satisfies the following two conditions

$$R_t^{-1}\overline{v}_t = \overline{v}_t^* \quad \text{and} \quad R_t R_t' = \Omega_t. \tag{8}$$

where R_t is invertible for all t. Then, it is clear that to identify the ith shock in $\overline{v}_t^*$, it is only necessary to restrict elements in the ith column of R_t. This is different from previous approaches in the empirical literature investigating the real effects of uncertainty shocks where the time-varying volatilities are modeled only after the structural level shocks are fully identified.

Imposing economic restrictions on the responses to the uncertainty shocks $\overline{v}_t^*$ involves conditions on the set of impulse response functions that we consider. To fix ideas, we first define our notion of an impulse response function. We use the generalized impulse response function of Koop et al. (1996). We distinguish between first moment impulse response

functions and second moment impulse response functions.

A *first moment impulse response function* gives the expected change in the conditional means of the observable variables from the jth uncertainty shock $\overline{v}_t^* = e_j$ conditional upon a previous volatility level σ_{t-1}^* (e_j is a column vector with a 1 in the jth element and zeros elsewhere). The dependence of the impulse response function on the rotation R_t is also made explicit.

$$\begin{aligned} &IRF_{t:t+S}[Y|\sigma_{t-1} = \sigma_{t-1}^*, \overline{v}_t^* = e_j; R_t] = \\ &\quad E(Y_{t:t+S}|\sigma_{t-1} = \sigma_{t-1}^*, \overline{v}_t^* = e_j; R_t) - E(Y_{t:t+S}|\sigma_{t-1} = \sigma_{t-1}^*, \overline{v}_t^* = 0; R_t) \end{aligned} \tag{9}$$

A *second moment impulse response function* gives the expected change in the variance covariance matrix of the innovations to the observable variables (ϵ_t) from the jth uncertainty shock $\overline{v}_t^* = e_j$ conditional upon a previous volatility level σ_{t-1}^*.

$$\begin{aligned} &IRF_{t:t+S}[\sigma|\sigma_{t-1} = \sigma_{t-1}^*, \overline{v}_t^* = e_j; R_t] = \\ &\quad E(\sigma_{t:t+S}|\sigma_{t-1} = \sigma_{t-1}^*, \overline{v}_t^* = e_j; R_t) - E(\sigma_{t:t+S}|\sigma_{t-1} = \sigma_{t-1}^*, \overline{v}_t^* = 0; R_t) \end{aligned} \tag{10}$$

These impulse response functions capture the expected effect on the first and second moments of a one standard deviation movement to the uncertainty shock of interest.

In both cases, the impulse response functions are conditional upon two state variables: the time $t-1$ level of volatility σ_{t-1}^* and the uncertainty shock $\overline{v}_t^*$. In addition to being the historical level of volatility, the time $t-1$ level of volatility σ_{t-1} also impacts the variance covariance matrix Ω_t of $\overline{v}_t$. Broadly speaking, a more volatile time period will in general imply larger volatility shocks. A benchmark we use is to set $\sigma_{t-1} = E[\sigma_t]$, which is the unconditional variance. We could also investigate the impulse response functions conditional on a high volatility time period (such as the Great Recession) or a low volatility time period (such as the Great Moderation).

These facts then suggest a straightforward procedure for restricting the set of impulse response functions we consider. The economic restrictions are restrictions on the set of impulse response functions following the jth uncertainty shock. Given a value σ_{t-1}^* that the researcher fixes beforehand, these restrictions imply restrictions on the admissible set of decompositions R_t. Finding the set of R_t that satisfies the conditions completes the procedure.

We will discuss computational aspects of the impulse response functions in a later section. First, we give concrete examples of how we impose sign restrictions.

2.3 Imposing sign restrictions in a simple model

In this subsection, we illustrate our identification strategy via examples. More specifically, we consider a 2-variable CAIW-in-VAR model and illustrate two different approaches to identify the real effects of uncertainty shocks: first moment and second moment restrictions. *First moment restrictions* impose conditions on the expected responses of the observed variables (Y_t) to an uncertainty shock. They involve restrictions on the first moment impulse response functions. *Second moment restrictions* impose conditions on the expected responses of the conditional variances and covariances of the innovations to the uncertainty shock. They involve restrictions on the second moment impulse response functions. It is important to note that although our examples only consider single first and second moment restrictions, our framework can handle both types of restrictions simultaneously, or multiples of either restriction.

2-variable CAIW-in-VAR model. Let us consider a simple 2-variable example.

$$\begin{pmatrix} y_{1,t} \\ y_{2,t} \end{pmatrix} = \Phi \begin{pmatrix} y_{1,t-1} \\ y_{2,t-1} \end{pmatrix} + Bf(\Sigma_t) + \begin{pmatrix} \epsilon_{1,t} \\ \epsilon_{2,t} \end{pmatrix}, \quad \begin{pmatrix} \epsilon_{1,t} \\ \epsilon_{2,t} \end{pmatrix} \Big| \underbrace{\begin{pmatrix} \Sigma_{11,t} & \Sigma_{12,t} \\ \Sigma_{12,t} & \Sigma_{22,t} \end{pmatrix}}_{\Sigma_t} \sim N\left(\begin{pmatrix} 0 \\ 0 \end{pmatrix}, \Sigma_t \right). \quad (11)$$

The volatility process is then

$$\begin{pmatrix} \Sigma_{11,t} \\ \Sigma_{12,t} \\ \Sigma_{22,t} \end{pmatrix} = \overline{C} + \overline{A} \begin{pmatrix} \Sigma_{11,t-1} \\ \Sigma_{12,t-1} \\ \Sigma_{22,t-1} \end{pmatrix} + \begin{pmatrix} \overline{v}_{11,t} \\ \overline{v}_{12,t} \\ \overline{v}_{22,t} \end{pmatrix}, \begin{pmatrix} \overline{v}_{11,t} \\ \overline{v}_{12,t} \\ \overline{v}_{22,t} \end{pmatrix} \sim \left(\begin{pmatrix} 0 \\ 0 \\ 0 \end{pmatrix}, \begin{pmatrix} \Omega_{11,t} & \Omega_{12,t} & \Omega_{13,t} \\ \Omega_{12,t} & \Omega_{22,t} & \Omega_{23,t} \\ \Omega_{13,t} & \Omega_{23,t} & \Omega_{33,t} \end{pmatrix} \right). \quad (12)$$

Example 1: Sign restriction on the second moment. A second moment restriction puts conditions on the expected movements of the conditional variances and covariances to the uncertainty shock. For example, one can consider the following restriction

> *The conditional variance of the innovation to $y_{1,t}$ increases in response to the uncertainty shock $\overline{v}^*_{1,t}$ contemporaneously (contemporaneous second moment restriction).*

Although we present a contemporaneous condition in this example, the sign restriction can be either contemporaneous or for multiple periods. The above restriction can be written in

$$E\left[\Sigma_{11,t+h}\middle|\begin{pmatrix}\Sigma_{11,t-1}\\ \Sigma_{12,t-1}\\ \Sigma_{22,t-1}\end{pmatrix}=E\left[\begin{pmatrix}\Sigma_{11,t}\\ \Sigma_{12,t}\\ \Sigma_{22,t}\end{pmatrix},\begin{pmatrix}\overline{v}^*_{1,t}\\ \overline{v}^*_{2,t}\\ \overline{v}^*_{3,t}\end{pmatrix}=\begin{pmatrix}1\\0\\0\end{pmatrix};R_t\right]-\right.$$
$$\left.E\left[\Sigma_{11,t+h}\middle|\begin{pmatrix}\Sigma_{11,t-1}\\ \Sigma_{12,t-1}\\ \Sigma_{22,t-1}\end{pmatrix}=E\left[\begin{pmatrix}\Sigma_{11,t}\\ \Sigma_{12,t}\\ \Sigma_{22,t}\end{pmatrix},\begin{pmatrix}\overline{v}^*_{1,t}\\ \overline{v}^*_{2,t}\\ \overline{v}^*_{3,t}\end{pmatrix}=\begin{pmatrix}0\\0\\0\end{pmatrix};R_t\right]>0,\quad \text{for } h=0.\right.$$

where we set the time $t-1$ value of volatility to its unconditional mean. There is no closed form for the set of admissible decompositions R_t. However, it is possible to obtain them through simulation-based methods as in Uhlig (2005) and Arias et al. (2014). Previous results in the sign restrictions literature (e.g. Uhlig, 2005) justifies us fixing $\widetilde{R}_t = chol(\Omega_t)$ and checking all possible rotation matrices Q, where $QQ' = Q'Q = I_3$. This is because any decomposition R_t can be written such that

$$R_t = \widetilde{R}_t Q. \tag{13}$$

We keep the rotations Q that satisfy the above second moment sign restriction.

Example 2: Sign restrictions on the first moment. A first moment restriction puts conditions on the expected responses of the observable variables to an uncertainty shock. First moment restrictions could help provide a sharper identification. For example, if it is suggested from economic theory the direction of an economic variable's movement following a certain source of uncertainty shock, imposing these restrictions could shrink the candidate uncertainty shocks. In this example, we consider a multi-step first moment restriction

> *The expected value of $y_{1,t}$ increases in response to the uncertainty shock $\overline{v}^*_{1,t}$ for the first H periods (multi-step first moment restriction).*

Again, this restriction can be written in terms of impulse response functions

$$E\left[y_{1,t+h}\middle|\begin{pmatrix}\Sigma_{11,t-1}\\ \Sigma_{12,t-1}\\ \Sigma_{22,t-1}\end{pmatrix}=E\left[\begin{pmatrix}\Sigma_{11,t}\\ \Sigma_{12,t}\\ \Sigma_{22,t}\end{pmatrix},\begin{pmatrix}\overline{v}^*_{1,t}\\ \overline{v}^*_{2,t}\\ \overline{v}^*_{3,t}\end{pmatrix}=\begin{pmatrix}1\\0\\0\end{pmatrix};R_t\right]-\right.$$
$$\left.E\left[y_{1,t+h}\middle|\begin{pmatrix}\Sigma_{11,t-1}\\ \Sigma_{12,t-1}\\ \Sigma_{22,t-1}\end{pmatrix}=E\left[\begin{pmatrix}\Sigma_{11,t}\\ \Sigma_{12,t}\\ \Sigma_{22,t}\end{pmatrix},\begin{pmatrix}\overline{v}^*_{1,t}\\ \overline{v}^*_{2,t}\\ \overline{v}^*_{3,t}\end{pmatrix}=\begin{pmatrix}0\\0\\0\end{pmatrix};R_t\right]>0,\quad \text{for } h=0,...,H,\right.$$

We can perform a simulation exercise similar to the previous example to find impulse response functions that satisfy the appropriate sign restrictions.

Sign restrictions implementation We discuss our simulation methodology to construct impulse response functions in a later section. Conditional upon being able to construct impulse response functions, implementing the sign restrictions algorithm is straightforward following the methodology of Uhlig (2005) or Arias et al. (2014). We draw the rotation matrix Q in equation 13 using a QR decomposition as in Arias et al. (2014) and keep the IRFs that satisfy the imposed sign restrictions.

2.4 Discussion on our choice of volatility process

In principle, we have multiple options for the form of our reduced-form volatility process. Modeling the reduced-form variance covariance matrix with the conditional autoregressive inverse Wishart process, however, leads to important advantages in implementing our approach. In this section, we lay out a key advantage of using our proposed volatility process in comparison to the popular model found in Primiceri (2005).

Primiceri (2005) models the volatility process Σ_t in the following fashion

$$
\begin{aligned}
\begin{pmatrix} \Sigma_{11,t} & \Sigma_{12,t} \\ \Sigma_{12,t} & \Sigma_{22,t} \end{pmatrix} &= \begin{pmatrix} 1 & 0 \\ \alpha_t & 1 \end{pmatrix} \begin{pmatrix} b_{1,t} & 0 \\ 0 & b_{2,t} \end{pmatrix} \begin{pmatrix} 1 & \alpha_t \\ 0 & 1 \end{pmatrix} \\
\begin{pmatrix} \log b_{1,t} \\ \log b_{2,t} \\ \alpha_t \end{pmatrix} &= \begin{pmatrix} \mu_{b_1} \\ \mu_{b_2} \\ \mu_\alpha \end{pmatrix} + \begin{pmatrix} \rho_{b_1} \log b_{1,t-1} \\ \rho_{b_2} \log b_{2,t-1} \\ \rho_\alpha \alpha_{t-1} \end{pmatrix} + \begin{pmatrix} \overline{v}^*_{\eta_{b_1},t} \\ \overline{v}^*_{\eta_{b_2},t} \\ \overline{v}^*_{\eta_\alpha,t} \end{pmatrix}, \\
\begin{pmatrix} \overline{v}^*_{\eta_{b_1},t} \\ \overline{v}^*_{\eta_{b_2},t} \\ \overline{v}^*_{\eta_\alpha,t} \end{pmatrix} &\sim N\left(\begin{pmatrix} 0 \\ 0 \\ 0 \end{pmatrix}, \begin{pmatrix} \zeta^2_{\eta_{b_1}} & 0 & 0 \\ 0 & \zeta^2_{\eta_{b_2}} & 0 \\ 0 & 0 & \zeta^2_{\eta_\alpha} \end{pmatrix} \right)
\end{aligned}
\tag{14}
$$

The Primiceri (2005) model is attractive in some respects. For example, if one assumes a Cholesky structure of the economy, the time-varying parameters can be nicely decomposed into volatility shocks $(b_{1,t}, b_{2,t})$ and smooth changes in the structure of the economy (α_t). Under this setting, the identification of uncertainty shocks comes through the Cholesky structure and interpretation of uncertainty innovations $\overline{v}^*_{\eta_{b_1},t}$, $\overline{v}^*_{\eta_{b_2},t}$, and $\overline{v}^*_{\eta_\alpha,t}$ are readily available. If one views the volatility model as a description of volatility dynamics, however, potentially coming from a non-Cholesky model economy, this interpretation does not hold.

That is, $\overline{v}^*_{\eta_{b_1},t}$, $\overline{v}^*_{\eta_{b_2},t}$, and $\overline{v}^*_{\eta_\alpha,t}$ are not structural uncertainty innovations anymore and the assumption that they are independent from each other may not be appropriate.

We can easily apply our framework to the volatility process laid out in Primiceri (2005). To study the effect of uncertainty shocks, we do not assume full identification of the VAR a priori. Instead, we use a flexible model for the forecast error variance-covariance matrix and then impose relevant restrictions directly on this volatility process to identify uncertainty shocks. One can adopt a flexible model for the volatility process in a similar way to equation 14,

$$\begin{pmatrix} \Sigma_{11,t} & \Sigma_{12,t} \\ \Sigma_{12,t} & \Sigma_{22,t} \end{pmatrix} = \begin{pmatrix} 1 & 0 \\ \alpha_t & 1 \end{pmatrix} \begin{pmatrix} b_{1,t} & 0 \\ 0 & b_{2,t} \end{pmatrix} \begin{pmatrix} 1 & \alpha_t \\ 0 & 1 \end{pmatrix}$$
$$\begin{pmatrix} \log b_{1,t} \\ \log b_{2,t} \\ \alpha_t \end{pmatrix} = \begin{pmatrix} \mu_{b_1} \\ \mu_{b_2} \\ \mu_\alpha \end{pmatrix} + A \begin{pmatrix} \log b_{1,t-1} \\ \log b_{2,t-1} \\ \alpha_{t-1} \end{pmatrix} + \begin{pmatrix} \overline{v}_{\eta_{b_1},t} \\ \overline{v}_{\eta_{b_2},t} \\ \overline{v}_{\eta_\alpha,t} \end{pmatrix}, \quad \begin{pmatrix} \overline{v}_{\eta_{b_1},t} \\ \overline{v}_{\eta_{b_2},t} \\ \overline{v}_{\eta_\alpha,t} \end{pmatrix} \sim N(0, \Omega) \tag{15}$$

where A and Ω are 3×3 matrices. Matrices A and Ω reflect the fact that the Cholesky structure might not be the model that we are aiming to analyze. The Cholesky structure is simply used to model the forecast error variance-covariance matrix, Σ_t, in a reduced-form manner. Then, identification of uncertainty shocks is done by imposing restrictions on Ω in conjunction with the assumption on the relationship between $\overline{v}_t$ and $\overline{v}^*_t$, $\overline{v}_t = R\overline{v}^*_t$ as in section 2.2. Under this modeling assumption, the identification strategy that we provided in the previous section is still applicable.

We prefer the CAIW model for practical reasons. As stated in Primiceri (2005), the estimated results from this decomposition are conditional upon the ordering of the variables. Therefore, in our simple example, flipping the order of $y_{1,t}$ and $y_{2,t}$ and reestimating the model will in theory lead to different results. In contrast, our conditional autoregressive inverse Wishart process does not suffer from this potential drawback. Furthermore, the autoregressive Wishart-type volatility specification is more parsimonious when compared to the full Primiceri (2005) specification. The Wishart process has $k^2 + \frac{k(k-1)}{2} + k + 1$ free parameters while the full Primiceri (2005) model has $k^2 + \frac{k(k-1)}{2} + 2k$ parameters.

2.5 Caveats

Even though we believe that our approach adds important tools to the macroeconomists' toolkit in analyzing the real effect of uncertainty shocks, we must also acknowledge some caveats. First, our approach does not allow level shocks to impact current uncertainty. This is an additional exclusion restriction that is implicitly assumed in our uncertainty shock

identification. Within our framework, it is complicated to allow this channel because our reduced-form covariance matrices (Σ_t) need to be positive definite. In the literature, this channel can be relaxed at the cost of full identification of all structural shocks (Creal and Wu, 2014) or the use of a proxy variable[6] (Bloom, 2009). Second, it is hard to find a case where our model exactly maps into a fully structural model such as a dynamic equilibrium model with time-varying volatilities or a classical structural VAR. Insofar as our econometric model is flexible and the economic restrictions we impose are limited, however, we believe our toolkit can aid in the discovery of important comovements in the data that more structural models with uncertainty shocks should be able to match.

3 Bayesian Analysis of CAIW-in-VAR Models

3.1 Posterior inference

Prior specification. As we take a Bayesian perspective, the presented CAIW-in-VAR model is completed by specifying prior distributions on the unknown parameters. Parameters in the conditional mean of the model, μ, Φ and B, are assumed to follow independent multivariate normal distributions,

$$\mu \sim N\left(m_\mu, V_\mu\right), \quad vec(\Phi) \sim N\left(m_\Phi, V_\Phi\right), \quad vec(B) \sim N\left(m_B, V_B\right)$$

where $vec(\cdot)$ is the vectorize operator. The choice of this prior specification facilitates posterior computation due to its conjugacy.

There are three types of parameters in the volatility equation (A, C, and ν). The parameter A governs the dynamic properties of the volatility matrix process. Each element of A follows an independent normal distribution except the element in the far upper-left corner. The prior distribution for the $(1,1)$-th element in the A matrix is set to be a truncated normal distribution defined on the positive real line to ensure identification (see Golosnoy et al. (2012) for more details),

$$\begin{aligned} A(1,1) &\sim TN(m_{A(1,1)}, V_{A(1,1)}, 0, \infty) \\ A(i,j) &\sim N(m_{A(i,j)}, V_{A(i,j)}) \quad \forall\,(i,j) \neq (1,1). \end{aligned}$$

[6] Recently, Carriero et al. (2015) pointed out that proxy variables in these VARs are subject to measurement error and could potentially lead to biased parameter estimates.

The parameter C determines the long-run mean of the volatility process. We set the prior for it as following an inverse Wishart distribution with scale matrix Ψ and degrees of freedom parameter df. As the Wishart-type distribution is quite a popular prior in the Bayesian literature for a variance covariance matrix, we believe it to be a natural choice for C,

$$C \sim IW\left(df, \Psi\right).$$

Finally, ν, the degrees of freedom parameter in the inverse Wishart process, follows a gamma distribution

$$\nu \sim Gamma(a_\nu, b_\nu)$$

where we truncate this distribution at $\nu > k + 3$ so that the inverse Wishart process is well defined and the variances of its elements exist.

Posterior simulator. We construct a Metropolis-within-Gibbs posterior simulator to draw from the posterior distribution of our parameters. The algorithm runs on the following cycles:

1. $p(\Sigma_t|\ others, Y)$ for $t = 0, 1, ..., T$: multivariate stochastic volatilities
2. $p(\mu, B, \Phi|\ others, Y)$: parameters in the conditional mean equation
3. $p(\nu|\ others, Y)$: degrees of freedom parameter in the inverse Wishart process
4. $p(C|\ others, Y)$: long-run mean parameter in the inverse Wishart process
5. $p(A|\ others, Y)$: dynamics parameter in the inverse Wishart process

where we define $p(\theta|others, Y)$ as the conditional distribution of θ given $Y_{1:T}$ and all other parameters except θ. In the appendix, we provide details of the algorithm with full conditional posterior distributions.

Our algorithm builds upon the specifications of Philipov and Glickman (2006) and Rinnergschwentner et al. (2011). Relative to their frameworks, our model has a complication in that the stochastic volatility appears in the conditional mean equation as well and therefore their posterior samplers are not directly applicable to our framework. Our algorithm adopts the single-move state simulator in the same spirit of Jacquier et al. (1994), which is widely used in the context of the stochastic volatility model (e.g., Cogley and Sargent, 2005; Clark, 2011, for macroeconomic applications).

3.2 Impulse response function

There are two types of impulse response functions that we consider, first moment impulse response functions and second moment impulse response functions. As we have the linear form for the volatilities in equation 6, calculating the second moment impulse response function is straightforward and no simulation methods are needed conditional upon a time $t-1$ volatility level and time t uncertainty shock. Calculating the first moment impulse response function to an uncertainty shock is complicated by the nonlinear nature of the system. Hence, conditional upon a parameter draw, we use simulation methods to compute the impulse response function.

Continuing with our 2-variable CAIW-in-VAR example in equation 11, we present how to calculate a first moment impulse response to an uncertainty shock. An extension to a larger dimension is possible without further complication.

Algorithm 1 *(IRF of the uncertainty shock of length S in the 2-variable CAIW-in-VAR model).*

1. *Choose initial value $\tilde{\Sigma}_{-1}$ for IRF, and set $m = 1$.*
2. *Consider 1 standard deviation increase of an element in $\overline{v}_0^*$ (here we present a 1 standard deviation increase of the third element in the vector $\overline{v}_0^*$),*

$$\overline{v}_0^{*,1} = \begin{pmatrix} 0 \\ 0 \\ 1 \end{pmatrix} \quad \textit{versus} \quad \overline{v}_0^{*,0} = \begin{pmatrix} 0 \\ 0 \\ 0 \end{pmatrix}.$$

3. *Form reduced-form shocks in the initial period $\overline{v}_0^1$ and $\overline{v}_0^0$. The matrix R_0 will depend on the identification scheme. As the third shock is operative, only the third column of R_0 must be identified.*

$$\overline{v}_0^1 = \begin{pmatrix} R_{13,0} \\ R_{23,0} \\ R_{33,0} \end{pmatrix} \quad \textit{versus} \quad \overline{v}_0^0 = \begin{pmatrix} 0 \\ 0 \\ 0 \end{pmatrix}.$$

4. *Simulate two volatility paths indexed by (m) (using equations 2 and 3) conditional on the initial shock and initial value $\tilde{\Sigma}_{-1}$,*

$$\{\Sigma_t^{(m)}(\overline{v}_0^1)\}_{t=0,\ldots,S} \quad \textit{versus} \quad \{\Sigma_t^{(m)}(\overline{v}_0^0)\}_{t=0,\ldots,S}.$$

5. *For each simulated volatility path, compute* $\{\overline{Y}_t^{(m)}(\overline{v}_0^{*,1})\}_{t=0,\ldots,S}$ *and* $\{\overline{Y}_t^{(m)}(\overline{v}_0^{*,0})\}_{t=0,\ldots,S}$ *implied by the volatility paths where* $\overline{Y}_t$ *is a mean conditional on* $\overline{Y}_{t-1}^{(m)}$ *and* $\Sigma_t^{(m)}$*:*

$$\overline{Y}_t^{(m)} = \widehat{\mu} + \widehat{\Phi}\overline{Y}_{t-1}^{(m)} + \widehat{B}f(\Sigma_t^{(m)}).$$

Go to step 4 with $m = m + 1$ *if* $m < M$*; otherwise go to step 6.*

6. *Form impulse response by integrating out the simulated volatility paths:*

$$IRF_{0:S}[Y_j|\tilde{\Sigma}_{-1}, \overline{v}_0^{*,1}; R_0] \approx \frac{1}{M}\sum_{m=0}^{M}\overline{Y}_{0:S}^{(m)}(\overline{v}_0^{*,1}) - \frac{1}{M}\sum_{m=0}^{M}\overline{Y}_{0:S}^{(m)}(\overline{v}_0^{*,0}).$$

Based on this algorithm, we can construct the posterior distributions for the IRFs of the uncertainty shocks. Sign-restricted IRFs require an additional simulation algorithm.

Algorithm 2 *(Posterior distribution sign-restricted IRFs).*

1. *Run the posterior sampler to obtain* S *draws from the posterior distribution of unknown parameters in the CAIW-in-VAR model.*
2. *For each posterior draw,* θ^s*, repeat the following* M *times,*
   (a) *Generate a candidate rotation matrix* R^* *by the QR decomposition.*
   (b) *Apply Algorithm 1 to obtain the impulse response function* $IRF_{0:S}[Y_j|\tilde{\Sigma}_{-1}, \overline{v}_0^{*,1}; R^*]$.[7]
3. *Among* $S \times M$ *IRFs, keep those that satisfy the sign restrictions.*

After running this algorithm, one obtains S^* draws of IRFs where $S^* < S \times M$. These draws form the posterior distribution of the IRFs, which can be used to construct point estimates and credible sets.

4 Empirical Application: The financial market and uncertainty shocks

Motivation. Since the Great Recession, a renewed interest has emerged on the role of the financial sector in macroeconomic fluctuations. Our empirical application investigates the relationship between the financial sector and uncertainty shocks. Heightened uncertainty could interfere with banks' willingness to lend, thereby disrupting efficient capital flows. This

[7] Not all R guarantee a positive definite volatility processes. We discard IRF draws that are based on non-positive definite volatility processes.

could be a potential channel through which the financial sector would transmit uncertainty to the real economy.

We view our empirical application as contributing to a fast growing literature on the relationship between the financial markets and the macroeconomy. Jermann and Quadrini (2012) and Christiano et al. (2014) find that shocks originating in the financial sector have significant macroeconomic effects. Fernandez-Villaverde and Rubio-Ramirez (2007) and Justiniano and Primiceri (2008) observe that volatility from shocks to the capital accumulation equation, which may be interpreted as financial sector shocks (e.g., Justiniano et al., 2011), are the main drivers of the time-varying volatility of macroeconomic fluctuations on U.S. data. Using proxies for uncertainty and financial conditions, Caldara et al. (2016) find that uncertainty shocks can lead to a significant recession only if they are transmitted through the financial channel. Ferreira (2014) isolates the importance of financial uncertainty and finds that it alone can account for 40% of the decline in GDP during the Great Recession.

This section is divided into two main parts. First, we discuss the empirical results using our econometric model[8]. Second, we present an exercise interpreting our empirical results through the lens of a structural model. Specifically, we show that a capital quality uncertainty shock produces comovements consistent with our identifying assumptions and results whereas a permanent TFP uncertainty shock does not. This exercise also shows that a reasonably calibrated dynamic equilibrium model does produce different comovements in observables following different sources of uncertainty shocks, justifying our sign restrictions identification approach.

Data. We use monthly data on log industrial production in the manufacturing sector, log consumer price index, the federal funds rate, and the excess bond premium from $1973M1 - 2012M12$. We obtained the macroeconomic data from the Federal Reserve Bank of St. Louis FRED and the excess bond premium data from Simon Gilchrist's website. Figure 1 displays the four monthly series.

Model and prior specification. We use a 4-variable specification of our CAIW-in-VAR model. Our preferred function linking the volatility to the mean portion of the model is $f(\Sigma_t) = \log\left(diag(\Sigma_t)\right)$[9]. We choose a VAR(12) for the conditional mean lag length, noting that this lag length essentially removes all autocorrelation from the fitted residuals in a model without stochastic volatility. For the CAIW process, we choose a lag length 1. In estimating

[8] In an appendix, we also compare our empirical findings to those from a VAR using two different proxies for uncertainty.

[9] We also tried $f(\Sigma_t) = diag(chol(\Sigma_t))$. Our results are robust to this specification.

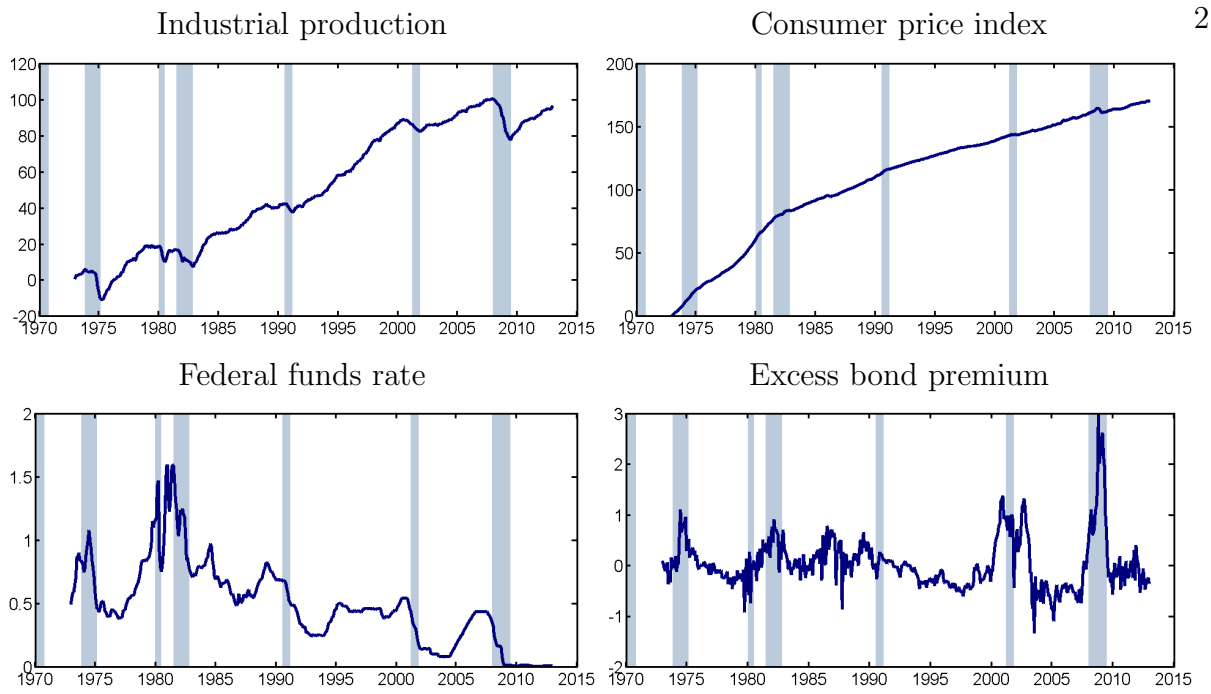


Figure 1 (Clockwise from top) Monthly log industrial production of the manufacturing sector, log consumer price index, federal funds rate, and excess bond premium (bottom) $1973M1 - 2012M12$. Blue bars indicate NBER recession dates.

the model, we take $100,000$ Markov chain Monte Carlo draws from our Metropolis-within-Gibbs sampler. We estimate all parameters in the model. Prior specifications can be found in the appendix. Estimates of the smoothed stochastic volatility process are also in the appendix.

Impulse response functions – restrictions. We consider the real effects of uncertainty shocks with and without a decline in financial sector conditions. To identify the two effects, we propose two different identification strategies. For both identifications, we set $\tilde{\Sigma}_{-1}$ to be the steady state volatility matrix.

Assumption $\mathcal{A}_u$ (Uncertainty shock only) The uncertainty shock, $\overline{v}_t$ satisfy $\mathcal{A}_u$:

$$\mathcal{A}_u : (E[\Sigma_{ii,h}|\sigma_{-1} = E(\sigma), \overline{v}_0^* = e_1; R_t] - E[\Sigma_{ii,h}|\sigma_{-1} = E(\sigma), \overline{v}_0^* = 0; R_t]) > 0 \text{ for } h = 0$$
$$\text{for } i = 1, ..., k.$$

The uncertainty shock only identification specifies that a $1-$ standard deviation uncertainty shock contemporaneously increases the volatility of all shocks hitting the economy, which is a second moment restriction. This identification of an uncertainty shock is similar in spirit to Jurado et al. (2015), which specifies that an uncertainty shock leads to an increase in the

volatilities of many economic series. This assumption imposes that we look at an aggregate uncertainty shock.

Assumption $\mathcal{A}_{uf}$ (Uncertainty shock transmitted through the financial sector) The uncertainty shock, $\overline{v}_t$, satisfy $\mathcal{A}_{uf,1}$ and $\mathcal{A}_{uf,2}$:

$$\mathcal{A}_{u,f,1}: \Big(E[\Sigma_{ii,h}|\tilde{\Sigma}_{-1} = E(\tilde{\Sigma}), \overline{v}_0^* = e_1; R_0] - E[\Sigma_{ii,h}|\tilde{\Sigma}_{-1} = E(\tilde{\Sigma}), \overline{v}_0^* = 0; R_0]\Big) > 0 \text{ for } h = 0$$
$$\text{for } i = 1, ..., k.$$
$$\mathcal{A}_{uf,2}: \Big(E[Y_{f,h}|\tilde{\Sigma}_{-1} = E(\tilde{\Sigma}), \overline{v}_0^* = e_1; R_0] - E[Y_{f,h}|\tilde{\Sigma}_{-1} = E(\tilde{\Sigma}), \overline{v}_0^* = 0; R_0]\Big) > 0$$
$$\text{for } h = 0, ..., H.$$

Relative to identification Assumption $\mathcal{A}_u$, identification Assumption $\mathcal{A}_{uf}$ additionally imposes that financial conditions worsen in expectation for H months. This is a first moment sign restriction. We set $H = 3$, meaning that we restrict financial conditions to worsen for 1 quarter. The motivation for this additional restriction are the empirical results by Caldara et al. (2016) and Ferreira (2014), which emphasize the importance of considering the financial sector when discussing the macroeconomic effects of uncertainty shocks.

Results from Assumption $\mathcal{A}_u$ (Uncertainty shock only). Consider the effects on the macroeconomy of an uncertainty shock (1 standard deviation increase) as shown in figures 2 and 3. Consistent with the sign restriction, the volatilities of all four variables increase in response to the uncertainty shock. The industrial production innovation volatility persists the longest. It stays elevated for around 12 months following the uncertainty shock. The CPI and excess bond premium innovation volatilities return to pre-shock levels after around half a year. The federal funds rate innovation volatility declines the quickest, only lasting for around 3 months. This increase in macroeconomic uncertainty has at best a marginal impact on the economy. There is some evidence of a decline in industrial production, but any marginally significant effect is quite transitory, disappearing after half a year. The maximal posterior median decline is -0.1%. Otherwise, there is little effect on any other variables. Overall, these results are consistent with uncertainty shocks having a small effect on the economy.

Results from Assumption $\mathcal{A}_{uf}$ (Uncertainty shock transmitted through the financial sector). We impose a further restriction that financial conditions worsen for 3 months following the increase in uncertainty. We interpret this restriction as identifying an increase in uncertainty that leads to a deterioration in financial conditions. This exercise

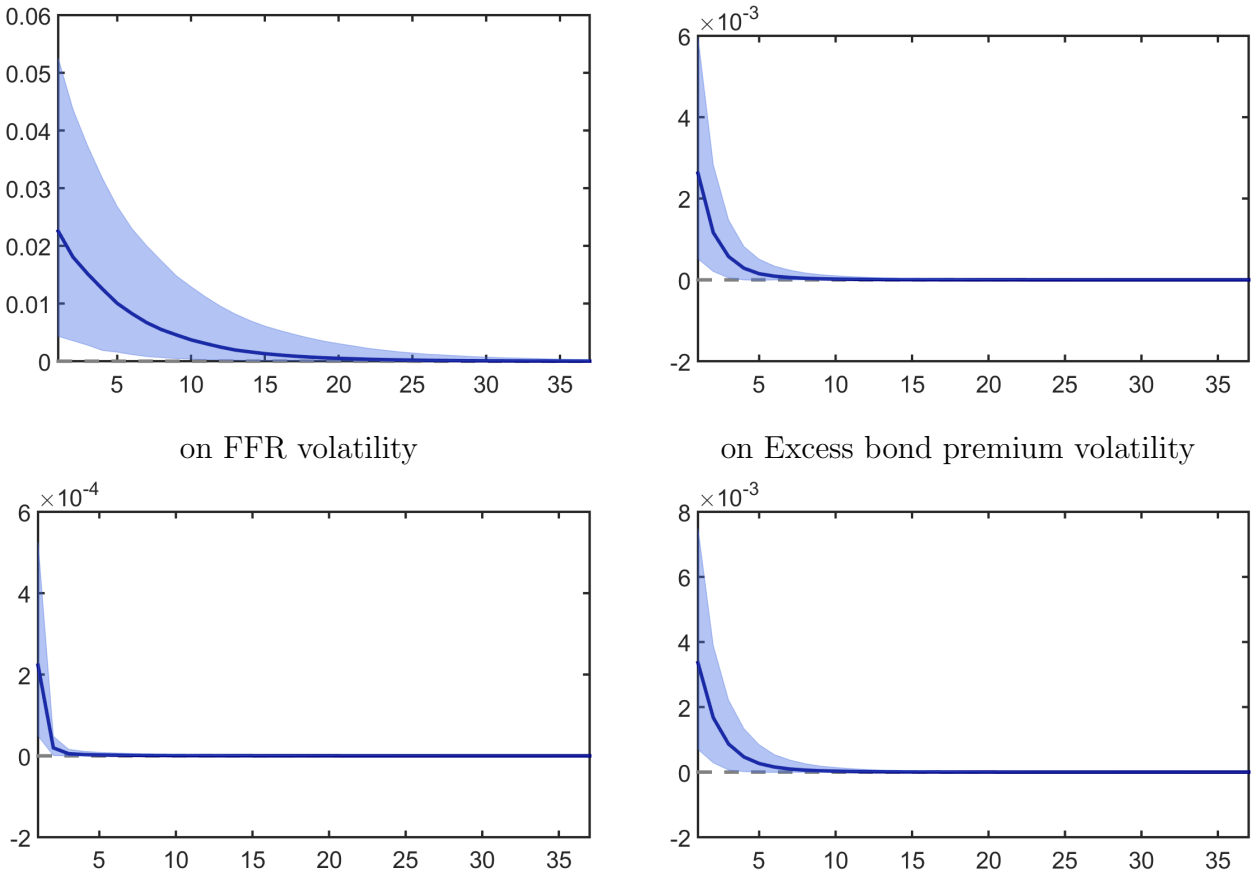


Figure 2 Effect of 1 standard deviation positive uncertainty shock with identification assumption $\mathcal{A}_u$ only. Dark lines give posterior median results. Bands indicate 80% posterior intervals. Time period is in months.

captures an effect similar to the one considered in Caldara et al. (2016). The results are presented in figure 4[10]. Upon restricting the uncertainty shock to move financial conditions, its impact on industrial production becomes more evident. Industrial production declines in a hump-shaped manner and the estimate's 80% credible band is below 0 for 15 months. Its maximal posterior decline increases relative to the earlier case as well, now reaching around -0.15%. These results are in line with Bloom (2009) in that an uncertainty shock leads to a hump-shaped response in industrial production. Relative to Bloom (2009), the decline in industrial production lasts longer by around 10 months and there is no evidence of a bounce-back effect. There is little evidence of any change in the price level or federal funds rate. The posterior median results show both series declining following the identified uncertainty

[10] Although in principle the additional sign restriction changes the set of admissable volatility responses, the figures for the volatility responses look quite similar between the two identification schemes. We believe it is more instructive to focus on the first moment responses so we suppress the volatility responses.

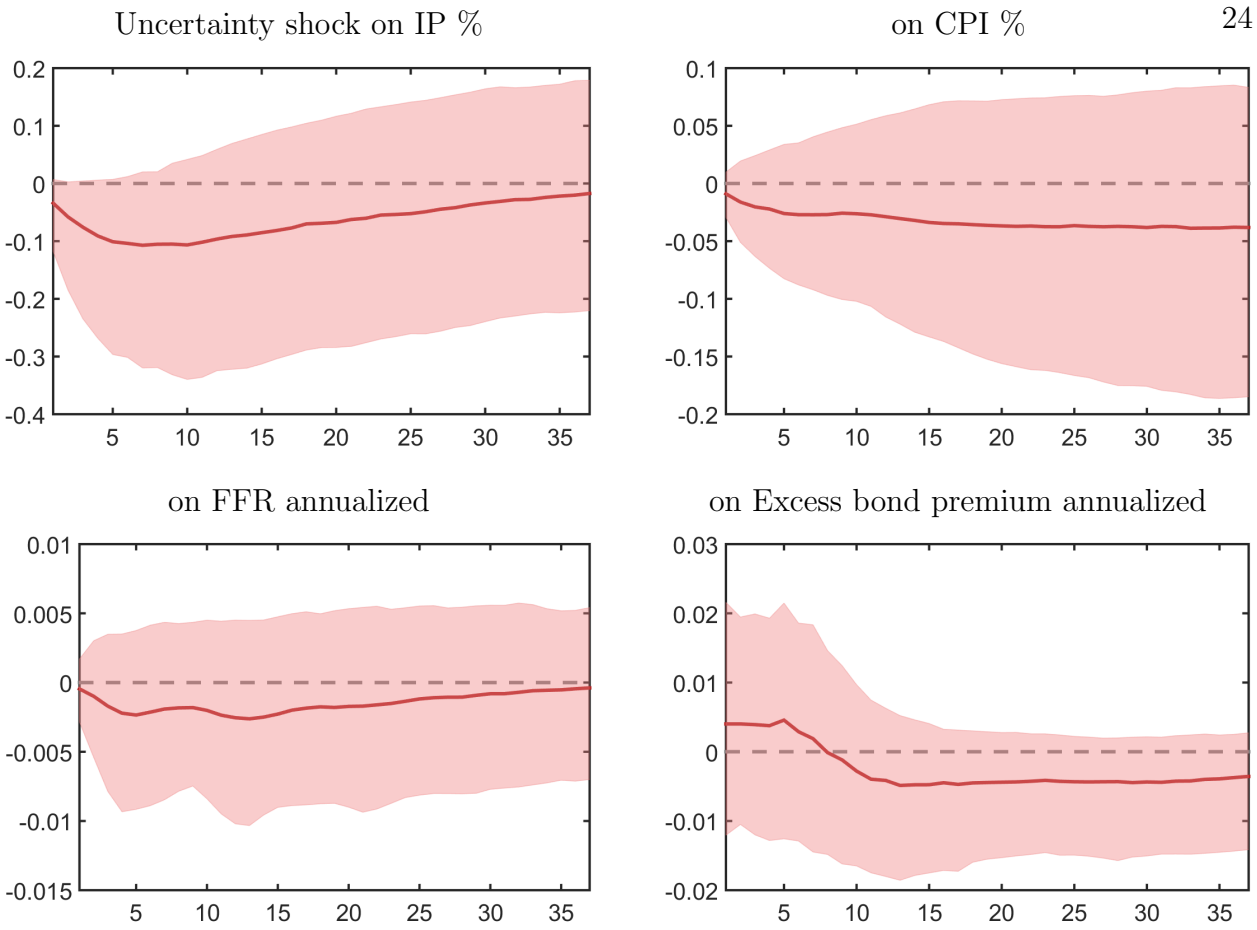


Figure 3 Effect of 1 standard deviation positive uncertainty shock with identification assumption $\mathcal{A}_u$ only. Dark lines give posterior median results. Bands indicate 80% posterior intervals. Time period is in months.

shock. Financial conditions continue to stay bad for around 4 months after the sign restriction ceases to hold. The excess bond premium increases by around 0.01% annualized. Its response is of a similar magnitude to the response of the excess bond premium to an uncertainty shock found in Caldara et al. (2016) when using more macro-based uncertainty proxies (such as forecast disagreement measures and the Economic Policy Uncertainty Index).

Structural model We investigate the likely structural sources of the comovements we identify with Assumption $\mathcal{A}_{uf}$ by specifying a dynamic equilibrium model with an explicit role for financial intermediaries, following Gertler and Karadi (2011). A key difference of our model relative to Gertler and Karadi (2011) is the utility function of the agents, which we have as Epstein-Zin in line with Basu and Bundick (2015). As the model is relatively standard in the literature, we leave the details of it to the appendix. We solve the model

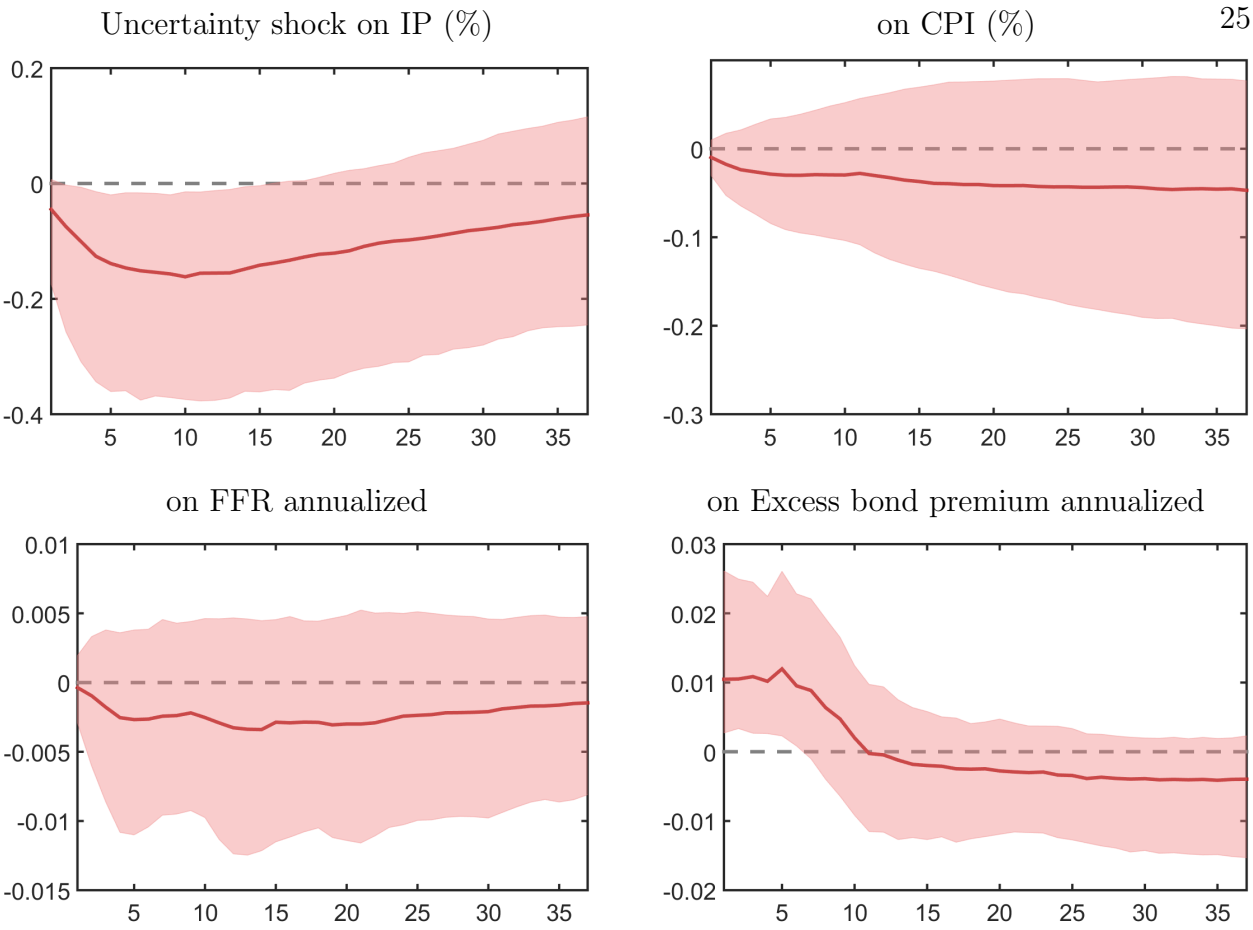


Figure 4 Effect of 1 standard deviation positive uncertainty shock with identification assumption $\mathcal{A}_{uf}$. Dark lines give posterior median results. Bands indicate 80% posterior intervals. Time period is in months.

using a third-order perturbation with pruning.

The model has two sources of volatility shocks: permanent TFP volatility and capital quality volatility. The TFP volatility shock captures macroeconomic uncertainty unrelated to the financial sector whereas capital quality volatility captures uncertainty originating in the financial sector. We ask the question whether real activity uncertainty or financial sector uncertainty is more likely to be transmitted through credit spreads. While our model is arguably stylized when compared to the full suite of shocks considered by Smets and Wouters (2007) and Justiniano et al. (2010), we view this exercise as an illustration of our methodology. Also, we would like to emphasize that a reasonably calibrated dynamic equilibrium model does produce different comovements in observable variables following different uncertainty shocks.

One important point of discussion is our choice of the utility function parameters. We

set risk aversion to be 10 and the intertemporal elasticity of substitution to be 0.8. The risk aversion parameter is standard in the literature, whereas we follow Basu and Bundick (2015) in calibrating the IES. This calibration of the IES implies that following an increase in TFP volatility, households consume less and save more due to the precautionary savings effect. We also choose the autoregressive persistence parameter of both volatility shocks to be 0.5, which implies that after one year, most of the increased volatility in the economy from a positive volatility shock has disappeared, consistent with our empirical results. The rest of the calibration is standard for a model specified at the quarterly frequency. Details can be found in the appendix.

As Born and Pfeifer (2014) discussed, there is a tension between generating large real effects from uncertainty shocks and unrealistically large effects from first moment shocks in dynamic equilibrium models. This is because many of the mechanisms that amplify uncertainty shocks also amplify first moment shocks. We view this issue as an important open question in the literature outside of the scope of this paper. Instead, we focus in this section on the directions of the impulse response functions and do not try to quantitatively match the responses. We use the same impulse response construction algorithms as in Fernandez-Villaverde et al. (2015) and Basu and Bundick (2015).

Let us first consider the implications of our first and second moment sign restrictions. Assumption $\mathcal{A}_{uf,1}$, which says that the conditional volatility of innovations to all variables in the vector autoregression increases on impact, is generated by both structural aggregate uncertainty shocks.

Assumption $\mathcal{A}_{uf,2}$, which says that the excess bond premium increases for 3 months following the uncertainty shock, rules out the permanent TFP uncertainty shock. As can be seen in figure 5, following a permanent TFP uncertainty shock, the spread between the return to capital and the risk free rate declines[11]. An increase in TFP uncertainty now makes investment in capital more attractive. The reason is with increased future uncertainty about TFP, a higher capital stock helps agents smooth out consumption, which encourages investment demand. The model does contain a moderate amount of nominal price rigidities, in line with Basu and Bundick (2015). Previous versions of that paper showed that with nominal price rigidities, it is possible to have both consumption and investment decline following a transitory TFP uncertainty shock through countercyclical markups. This effect is still present in our model. The main difference is that with a permanent TFP uncertainty shock in our model as opposed to a transitory TFP uncertainty shock, the precautionary savings channel is much stronger. While overall investment still declines following the uncertainty shock,

[11]This spread is the closest match to the excess bond premium in the context of the model.

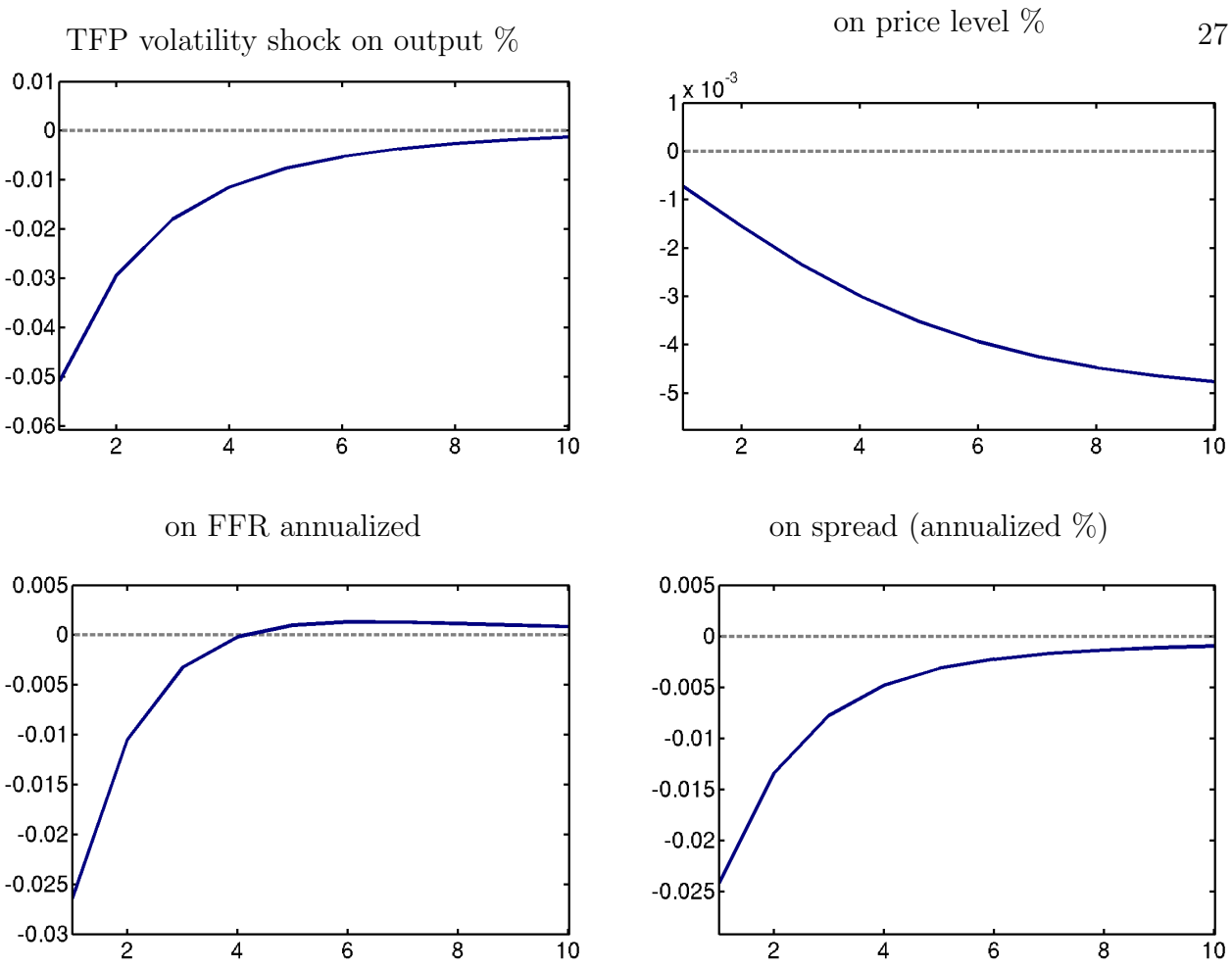


Figure 5 Effect of 1 standard deviation positive TFP volatility shock. Model time period is in quarters.

investment net of capital replacement goes up because the utilization of capital declines as well, which lowers the amount of capital depreciation. In the Gertler and Karadi (2011) model, it is movements in net investment that is relevant for the price of capital. Overall, the price of capital increases and the expected return to capital declines. The financial accelerator effect works in opposite, as the increase in the price of capital loosens the balance sheet constraints of the banks. This makes the overall effect of the uncertainty shock on the economy milder.

The results shown in figure 6 provide evidence that uncertainty originating in the financial sector, as opposed to uncertainty from real activity, is more likely to be the source of volatility that leads to a deterioration of financial conditions. Uncertainty about future capital quality increases the riskiness of investment. This channel greatly decreases the incentive to invest, which causes net investment to decline even with a decline in utilization. The decline in net

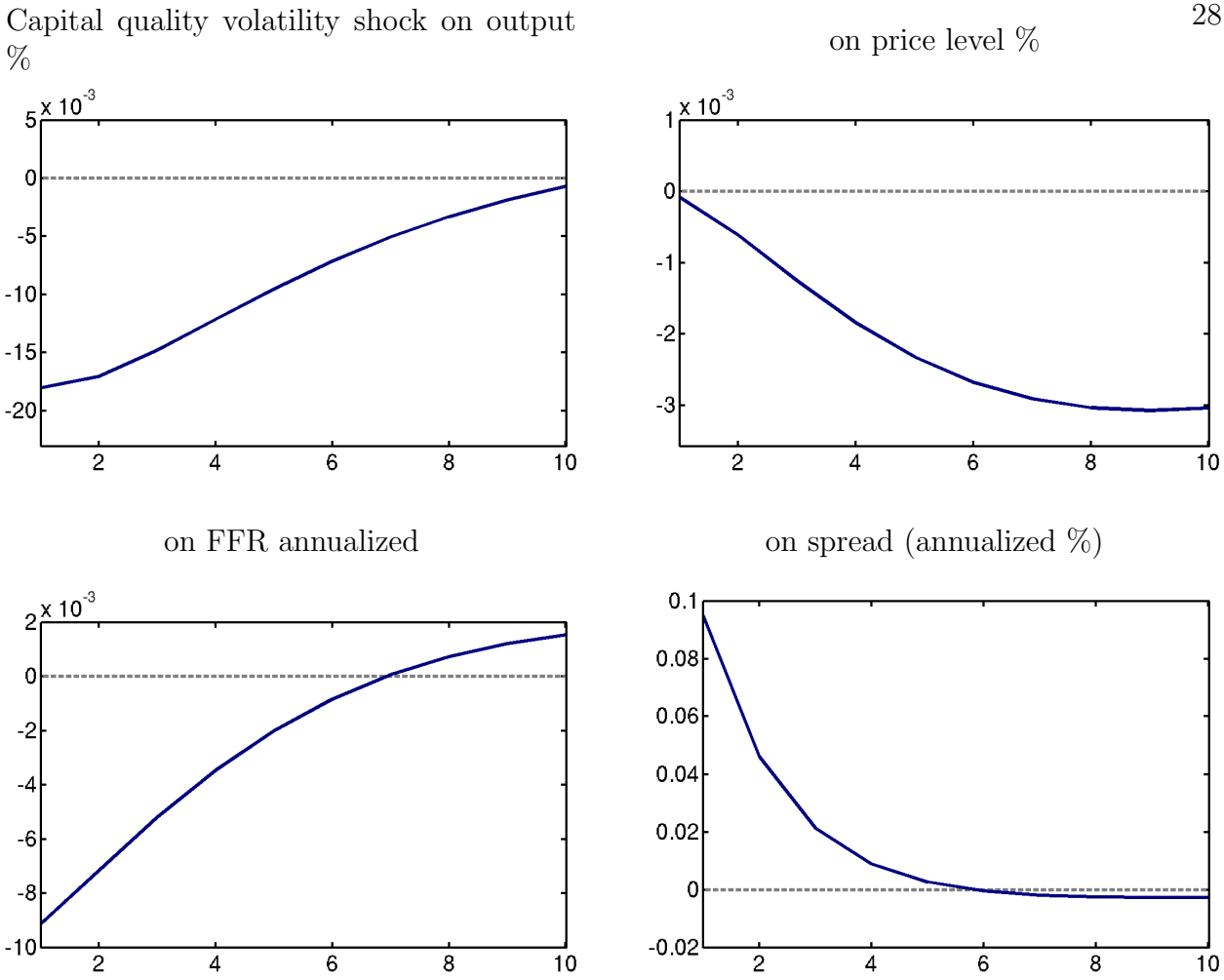


Figure 6 Effect of 1 standard deviation positive capital quality volatility shock. Model time period is in quarters.

investment leads to a decline in the price of capital, an increase in spreads, and a tightening of intermediary balance sheets. The financial accelerator effect amplifies the downturn, leading to a fall in aggregate demand and a decrease in output and inflation.

It is important to remember that these sign restriction assumptions on the econometric model are conditions imposed by the researcher. In this example, the first moment restriction has imposed an important identifying restriction. Imposing more sign restrictions generally decreases the set of structural uncertainty shocks consistent with the restrictions.

5 Conclusion and Future direction

We have advanced the conditional autoregressive inverse Wishart-in-vector autoregression model to evaluate the real effects of uncertainty shocks. We discuss a novel empirical strategy to analyze uncertainty shocks through the first and second moment responses they produce. The strategy allows for the imposition of a limited number of economic restrictions on the uncertainty shocks, thus potentially limiting concerns of misspecification. The paper also presents algorithms to construct impulse response functions to uncertainty shocks. In an empirical application, we evaluate the importance of the financial sector in transmitting uncertainty shocks to the macroeconomy. Our results show that financial conditions are important in transmitting uncertainty shocks to the real economy. Specifically, our preferred identification assumptions for an uncertainty shock transmitted through the financial sector lead to industrial production declining by -0.15% following a one standard deviation rise in uncertainty. Interpreting the results through the lens of a calibrated dynamic equilibrium model, the uncertainty shock we identify likely originates in the financial sector.

References

Arias, J., J. F. Rubio-Ramírez, and D. F. Waggoner (2014): "Inference Based on SVARs Identified with Sign and Zero Restrictions: Theory and Applications," .

Atchadé, Y. F. and J. S. Rosenthal (2005): "On Adaptive Markov Chain Monte Carlo Algorithms," *Bernoulli*, 11, 815–828.

Bachmann, R., S. Elstner, and E. Sims (2013): "Uncertainty and Economic Activity: Evidence from Business Survey Data," *American Economic Journal: Macroeconomics*, 5, 217–249.

Baker, S., N. Bloom, and S. Davis (2013): "Measuring Economic Policy Uncertainty," Tech. rep., policyuncertainty.com.

Basu, S. and B. Bundick (2015): "Uncertainty Shocks in a Model of Effective Demand," Boston College Working Papers in Economics 774, Boston College Department of Economics.

Baumeister, C. and J. D. Hamilton (2015): "Sign Restrictions, Structural Vector Autoregressions, and Useful Prior Information," *Econometrica*, 83, 1963–1999.

Baumeister, C. and G. Peersman (2013): "Time-Varying Effects of Oil Supply Shocks on the US Economy," *American Economic Journal: Macroeconomics*, 5, 1–28.

Bloom, N. (2009): "The Impact of Uncertainty Shocks," *Econometrica*, 77, 623–685.

——— (2014): "Fluctuations in Uncertainty," *Journal of Economic Perspectives*, 28, 153–176.

Born, B. and J. Pfeifer (2014): "Policy Risk and the Business Cycle," *Journal of Monetary Economics*, 68, 68–85.

Caldara, D., C. Fuentes-Albero, S. Gilchrist, and E. Zakrajsek (2016): "On the Identification of Financial and Uncertainty Shocks," *European Economic Review*, forthcoming.

Carriero, A., T. Clark, and M. Marcellino (2016): "Measuring Uncertainty and Its Impact on the Economy," *Working paper*.

Carriero, A., H. Mumtaz, K. Theodoridis, and A. Theophilopoulou (2015): "The Impact of Uncertainty Shocks under Measurement Error. A Proxy SVAR approach," *Journal of Money, Credit and Banking*.

Christiano, L. J., R. Motto, and M. Rostagno (2014): "Risk Shocks," *American Economic Review*, 104, 27–65.

Clark, T. E. (2011): "Real-Time Density Forecasts from Bayesian Vector Autoregressions with Stochastic Volatility," *Journal of Business & Economic Statistics*, 29.

Cogley, T. and T. J. Sargent (2005): "Drift and Volatilities: Monetary Policies and Outcomes in the Post WWII U.S," *Review of Economic Dynamics*, 8, 262–302.

Creal, D. D. and J. C. Wu (2014): "Interest Rate Uncertainty and Economic Fluctuations," NBER Working Papers 20594, National Bureau of Economic Research, Inc.

Domowitz, I. and C. S. Hakkio (1985): "Conditional variance and the risk premium in the foreign exchange market," *Journal of International Economics*, 19, 47–66.

Elder, J. (2004): "Another Perspective on the Effects of Inflation Uncertainty," *Journal of Money, Credit and Banking*, 36, 911–28.

Elder, J. and A. Serletis (2010): "Oil Price Uncertainty," *Journal of Money, Credit and Banking*, 42, 1137–1159.

Engle, R. F., D. M. Lilien, and R. P. Robins (1987): "Estimating Time Varying Risk Premia in the Term Structure: The Arch-M Model," *Econometrica*, 55, 391–407.

Fernandez-Villaverde, J., P. Guerron-Quintana, K. Kuester, and J. Rubio-Ramirez (2015): "Fiscal Volatility Shocks and Economic Activity," Tech. Rep. 11.

Fernandez-Villaverde, J., P. Guerron-Quintana, J. F. Rubio-Ramirez, and M. Uribe (2011): "Risk Matters: The Real Effects of Volatility Shocks," *American Economic Review*, 101, 2530–61.

Fernandez-Villaverde, J. and J. F. Rubio-Ramirez (2007): "Estimating Macroeconomic Models: A Likelihood Approach," *Review of Economic Studies*, 74, 1059–1087.

Ferreira, R. (2014): "Financial Volatility and its Economic Effects," .

Foerster, A. T. (2015): "Financial Crises, Unconventional Monetary Policy Exit Strategies, and Agents' Expectations," *Journal of Monetary Economics*, 76, 191–207.

Fox, E. B. and M. West (2013): "Autoregressive Models for Variance Matrices: Stationary Inverse Wishart Processes," Tech. rep.

French, K. R., G. W. Schwert, and R. F. Stambaugh (1987): "Expected Stock Returns and Volatility," *Journal of Financial Economics*, 19, 3–29.

Gertler, M. and P. Karadi (2011): "A Model of Unconventional Monetary Policy," *Journal of Monetary Economics*, 58, 17–34.

Gilchrist, S. and E. Zakrajsek (2012): "Credit Spreads and Business Cycle Fluctuations," *American Economic Review*, 102, 1692–1720.

Golosnoy, V., B. Gribisch, and R. Liesenfeld (2012): "The Conditional Autoregressive Wishart Model for Multivariate Stock Market Volatility," *Journal of Econometrics*, 167, 211–223.

Gourieroux, C., J. Jasiak, and R. Sufana (2009): "The Wishart Autoregressive Process of Multivariate stochastic Volatility," *Journal of Econometrics*, 150, 167–181.

Jacquier, E., N. G. Polson, and P. E. Rossi (1994): "Bayesian Analysis of Stochastic Volatility Models," *Journal of Business & Economic Statistics*, 12, 371–89.

Jermann, U. and V. Quadrini (2012): "Macroeconomic Effects of Financial Shocks," *American Economic Review*, 102, 238–71.

Jo, S. (2014): "The Effects of Oil Price Uncertainty on Global Real Economic Activity," *Journal of Money, Credit and Banking*, 46, 1113–1135.

Jurado, K., S. C. Ludvigson, and S. Ng (2015): "Measuring Uncertainty," *American Economic Review*, 105, 1177–1216.

Justiniano, A., G. Primiceri, and A. Tambalotti (2011): "Investment Shocks and the Relative Price of Investment," *Review of Economic Dynamics*, 14, 101–121.

Justiniano, A. and G. E. Primiceri (2008): "The Time-Varying Volatility of Macroeconomic Fluctuations," *American Economic Review*, 98, 604–41.

Justiniano, A., G. E. Primiceri, and A. Tambalotti (2010): "Investment shocks and business cycles," *Journal of Monetary Economics*, 57, 132–145.

Karapanagiotidis, P. (2012): "Improving Bayesian VAR Density Forecasts through Autoregressive Wishart Stochastic Volatility," MPRA Paper 38885, University Library of Munich, Germany.

Koop, G., M. H. Pesaran, and S. M. Potter (1996): "Impulse Response Analysis in Nonlinear Multivariate Models," *Journal of Econometrics*, 74, 119–147.

Koopman, S. J. and E. H. Uspensky (2002): "The Stochastic Volatility in Mean Model: Empirical Evidence from International Stock Markets," *Journal of Applied Econometrics*, 17, 667–689.

Leduc, S. and Z. Liu (2012): "Uncertainty Shocks Are Aggregate Demand Shocks," Working Paper Series 2012-10, Federal Reserve Bank of San Francisco.

Ludvigson, S. C., S. Ma, and S. Ng (2015): "Uncertainty and Business Cycles: Exogenous Impulse or Endogenous Response?" NBER Working Papers 21803, National Bureau of Economic Research, Inc.

Montes-Galdon, C. (2015): "Estimating Volatility Shocks," Tech. rep., Columbia University.

Mumtaz, H. and K. Theodoridis (2016): "The Changing Transmission of Uncertainty Shocks in the US: An Empirical Analysis," *Journal of Business & Economic Statistics*, forthcoming.

Mumtaz, H. and F. Zanetti (2013): "The Impact of the Volatility of Monetary Policy Shocks," *Journal of Money, Credit and Banking*, 45, 535–558.

Philipov, A. and M. E. Glickman (2006): "Multivariate Stochastic Volatility via Wishart Processes," *Journal of Business & Economic Statistics*, 24, 313–328.

Primiceri, G. E. (2005): "Time Varying Structural Vector Autoregressions and Monetary Policy," *Review of Economic Studies*, 72, 821–852.

Rinnergschwentner, W., G. Tappeiner, and J. Walde (2011): "Multivariate Stochastic Volatility via Wishart Processes - A Continuation," Working Papers 2011-19, Faculty of Economics and Statistics, University of Innsbruck.

Rotemberg, J. J. (1982): "Sticky Prices in the United States," *Journal of Political Economy*, 90, 1187–1211.

Rubio-Ramirez, J., W. D. F., and T. Zha (2010): "Structural Vector Autoregressions: Theory of Identification and Algorithms for Inference," *Review of Economic Studies*, 77, 665–696.

Schorfheide, F., D. Song, and A. Yaron (2016): "Identifying Long-Run Risks: A Bayesian Mixed-Frequency Approach," Tech. rep., University of Pennsylvania.

Scotti, C. (2013): "Surprise and Uncertainty Indexes: Real-Time Aggregation of Real-Activity Macro Surprises," International Finance Discussion Papers 1093, Board of Governors of the Federal Reserve System (U.S.).

Sims, C. A. and T. Zha (2006): "Were There Regime Switches in U.S. Monetary Policy?" *American Economic Review*, 96, 54–81.

Smets, F. and R. Wouters (2007): "Shocks and Frictions in US Business Cycles: A Bayesian DSGE Approach," *American Economic Review*, 97, 586–606.

Uhlig, H. (1997): "Bayesian Vector Autoregressions With Stochastic Volatility," *Econometrica*, 59–73.

——— (2005): "What Are the Effects of Monetary Policy on Output? Results from An Agnostic Identification Procedure," *Journal of Monetary Economics*, 52, 381–419.

Appendix

A Details of the posterior sampler

The algorithm runs on the following cycles:

1. $p(\Sigma_0|\ others)$: Multivariate stochastic volatility at the initial period.
2. $p(\Sigma_t|\ others)$ for $t = 1, ..., T$: Multivariate stochastic volatilities.
3. $p(\Sigma_T|\ others)$: Multivariate stochastic volatility at the last period.
4. $p(\mu, B, \Phi|\ others)$: Parameter in the conditional mean equation.
5. $p(\nu|\ others)$: Parameter in Wishart process.
6. $p(C|\ others)$: Parameter in Wishart process.
7. $p(A|\ others)$: Parameter in Wishart process.

where $p(\theta|others)$ means the conditional distribution of θ given $Y_{1:T}$ and all other parameters except θ. We denote the previous draw as θ^{old}. Note that the joint posterior distribution is

$$p(\mu, B, \Phi, \nu, C, A, \Sigma_{0:T}|Y_{1:T}) \propto p(Y_{1:T}|\mu, B, \Phi, \Sigma_{1:T})p(\Sigma_{1:T}|\nu, C, A, \Sigma_0)p(\mu, B, \Phi, \nu, C, A, \Sigma_0)$$

where the likelihood function can be decomposed as

$$p(Y_{1:T}|\mu, B, \Phi, \Sigma_{1:T}) = \prod_{t=1}^{T} p(Y_t|Y_{t-1}, \mu, B, \Phi, \Sigma_t),$$

where we implicitly conditioned on first p observations, $Y_0 = [y_0, y_{-1}, ..., y_{(p-1)}]$. p is the number of lags included in the VAR. To be able to construct an efficient MCMC sampling algorithm, we break the joint posterior into multiple blocks. For example, the conditional posterior distribution for the multivariate stochastic volatility is decomposed into the following pieces,

$$p(\Sigma_{1:T}|\nu, C, A, \Sigma_0, Y_{1:T}) = \left(\prod_{t=1}^{T} p(\Sigma_t|\Sigma_{t-1}, \nu, C, A, Y_t) \right)$$

and iteratively sample Σ_t from $t = 1$ to $t = T$.

Step 1: $\boldsymbol{\Sigma_0}$ We assume that the prior distribution of the initial covariance matrix as

$$\Sigma_0 \sim IW(v_0, V_0^{-1}), \quad V_0 = \frac{1}{v_0 - k - 1}\left\{(I - \overline{A})^{-1}\overline{C}\right\}^{-1}.$$

This prior specification assumes that Σ_0 is centered around the long-run mean of Σ_t. v_0 is an additional hyperparameter and we fix it to some number. The conditional posterior distribution of Σ_0 can be written as

$$p(\Sigma_0|others) \propto p(\Sigma_1|\Sigma_0, others')p(\Sigma_0|others')$$

where $others$ is $\Theta_{(-\Sigma_0)}$ and $others'$ is $\Theta_{(-\Sigma_0,-\Sigma_1)}$. Relevant terms are

$$p(\Sigma_1|\Sigma_0, others') \propto |S_0|^{-\nu/2}\exp\left(-\frac{1}{2}trace(S_0^{-1}\Sigma_1^{-1})\right)$$

and

$$p(\Sigma_0|others') \propto |\Sigma_0|^{-\frac{v_0+k+1}{2}}\exp\left(-\frac{1}{2}trace(V_0^{-1}\Sigma_0^{-1})\right).$$

We generate draws from the conditional distribution of Σ_0 by the random-walk-like proposal distribution with the following proposal distribution,

$$\Sigma_0^* \sim IW(\widetilde{w}_0 + k + 1, \widetilde{w}_0\Sigma_0^{old})$$

where $\widetilde{w}_0$ is a tuning parameter which governs the variance of the proposal distribution. High $\widetilde{w}_0$ leans to less variable proposal distribution. As is usual random walk MH algorithm, this proposal distribution is centered on previous draw, Σ_0^{old}. However, the proposal density is not symmetric. The acceptance ratio is then,

$$\begin{aligned}
\widetilde{r}_{\Sigma_0} &= \left\{\frac{p(\Sigma_1|\Sigma_0^*, others')p(\Sigma_0^*|others')/q(\Sigma_0^*|\Sigma_0^{old})}{p(\Sigma_1|\Sigma_0^{old}, others')p(\Sigma_0^{old}|others')/q(\Sigma_0^{old}|\Sigma_0^*)}, 1\right\} \\
&= \left\{\frac{p(\Sigma_1|\Sigma_0^*, others')p(\Sigma_0^*|others')}{p(\Sigma_1|\Sigma_0^{old}, others')p(\Sigma_0^{old}|others')}\left(\frac{|\Sigma_t^*|}{|\Sigma_t^{old}|}\right)^{\frac{(2\widetilde{w}+3k+3)}{2}} \quad ... \right. \\
&\qquad \left. ... \times \exp\left(-\frac{\widetilde{w}}{2}tr\left(-\Sigma_t^{old}(\Sigma_t^*)^{-1} + \Sigma_t^*(\Sigma_t^{old})^{-1}\right)\right), 1\right\}.
\end{aligned}$$

Step 2: Σ_t for $t = 1, 2, ..., T-1$ The conditional posterior is

$$\begin{aligned} p(\Sigma_t|others) \propto & |\Sigma_t|^{-(\nu+k+1)/2} \exp\left(-\frac{1}{2} tr(S_{t-1}^{-1}\Sigma_t^{-1})\right) \\ & \times |\Sigma_t|^{-1/2} \exp\left(-\frac{1}{2} tr\left(\epsilon_t' \Sigma_t^{-1} \epsilon_t\right)\right) \\ & \times |S_t|^{-\nu/2} \exp\left(-\frac{1}{2} tr\left(S_t^{-1}\Sigma_{t+1}^{-1}\right)\right) \end{aligned}$$

where we write

$$\epsilon_t = \underbrace{Y_t - \mu - \Phi Y_{t-1}}_{=e_t} - Bf(\Sigma_t) = e_t - Bf(\Sigma_t).$$

Then, we re-write the conditional posterior as

$$\begin{aligned} p(\Sigma_t|others) \propto & IW(\Sigma_t|\nu, \widetilde{S}_{t-1}^{-1}) \quad : \text{proposal density} \\ & \times |\Sigma_t|^{-1/2}|S_t|^{-\nu/2} \exp\left(-\frac{1}{2} tr\left(S_t^{-1}\Sigma_{t+1}^{-1}\right)\right) \quad : \text{MH correction 1} \\ & \times \exp\left(-\frac{1}{2} tr\Big(\left[-2e_t g(\Sigma_t)' + g(\Sigma_t)g(\Sigma_t)'\right]\Sigma_t^{-1}\Big)\right) \quad : \text{MH correction 2} \end{aligned}$$

where

$$g(\Sigma_t) = Bf(\Sigma_t) \quad \text{and} \quad \widetilde{S}_{t-1} = \left(S_{t-1}^{-1} + e_t e_t'\right)^{-1}.$$

We draw Σ_t based on the independent Metropolis-Hastings algorithm with the inverse Wishart distribution as a proposal distribution, $\Sigma_t^* \sim IW\left(\nu, \widetilde{S}_{t-1}^{-1}\right)$. The acceptance ratio is then,

$$r_{\Sigma_t} = \left\{ \frac{|\Sigma_t^*|^{-1/2}|S_t^*|^{-\nu/2} \exp\Big(-\frac{1}{2} tr\Big((S_t^*)\Sigma_{t+1}^{-1}\Big)\Big) \exp\Big(-\frac{1}{2} tr\Big(\left[-2e_t g(\Sigma_t^*)' + g(\Sigma_t^*)g(\Sigma_t^*)'\right](\Sigma_t^*)^{-1}\Big)\Big)}{|\Sigma_t^{old}|^{-1/2}|S_t^{old}|^{-\nu/2} \exp\Big(-\frac{1}{2} tr\Big((S_t^{old})\Sigma_{t+1}^{-1}\Big)\Big) \exp\Big(-\frac{1}{2} tr\Big(\left[-2e_t g(\Sigma_t^{old})' + g(\Sigma_t^{old})g(\Sigma_t^{old})'\right](\Sigma_t^{old})^{-1}\Big)\Big)}, 1 \right\}$$

and we set $\Sigma_t^{new} = \Sigma_t^*$ with probability $\min(r_{\Sigma_t}, 1)$, $\Sigma_t^{new} = \Sigma_t^{old}$ otherwise.

We also consider the random-walk-like proposal distribution with the following proposal distribution,

$$\Sigma_t^* \sim IW(\widetilde{w} + k + 1, \widetilde{w}\Sigma_t^{old})$$

where $\widetilde{w}$ is a tuning parameter which governs the variance of the proposal distribution. High $\widetilde{w}$ leads to less variable proposal distribution. We set $\widetilde{w} = 100$, which results in 20%$\sim$30% acceptance rates for each Σ_t. As in usual random walk MH algorithm, this proposal distribution is centered on previous draw, Σ_t^{old}. However, the proposal density is

not symmetric. The acceptance ratio is then,

$$\begin{aligned}\widetilde{r}_{\Sigma t} &= \left\{ \frac{p(\Sigma_t^*|others)/q(\Sigma_t^*|\Sigma_t^{old})}{p(\Sigma_t^{old}|others)/q(\Sigma_t^{old}|\Sigma_t^*)}, 1 \right\} \\ &= \left\{ \frac{p(\Sigma_t^*|others)}{p(\Sigma_t^{old}|others)} \left(\frac{|\Sigma_t^*|}{|\Sigma_t^{old}|} \right)^{\frac{(2\widetilde{w}+3k+3)}{2}} \exp\left(-\frac{\widetilde{w}}{2} tr\left(-\Sigma_t^{old}(\Sigma_t^*)^{-1} + \Sigma_t^*(\Sigma_t^{old})^{-1} \right) \right), 1 \right\}.\end{aligned}$$

In our application, we set our proposal distribution as a mixture of above two proposal distributions. More specifically, we propose a candidate draw, Σ_t^*:

$$\Sigma_t^* \sim \begin{cases} IW(\nu, \widetilde{S}_{t-1}^{-1}) & \text{with probability } p_\Sigma \\ IW(\widetilde{w}+k+1, \widetilde{w}\Sigma_t^{old}) & \text{with probability } (1-p_\Sigma). \end{cases}$$

Step 3: $\boldsymbol{\Sigma_T}$ The full conditional posterior is

$$\begin{aligned} p(\Sigma_T|others) &\propto |\Sigma_T|^{-(\nu+k+1)/2} \exp\left(-\frac{1}{2} tr\left(S_{T-1}^{-1}\Sigma_T^{-1} \right) \right) \times |\Sigma_T|^{-1/2} \exp\left(-\frac{1}{2}\epsilon_T'\Sigma_T^{-1}\epsilon_T \right) \\ &\propto |\Sigma_T|^{-(\nu+k+1)/2} \exp\left(-\frac{1}{2} tr\left(S_{T-1}^{-1}\Sigma_T^{-1} \right) \right) \times |\Sigma_T|^{-1/2} \exp\left(-\frac{1}{2}e_T'\Sigma_T^{-1}e_T \right) \\ &\quad \times \exp\left(-\frac{1}{2}\left(\epsilon_T'\Sigma_T^{-1}\epsilon_T - e_T'\Sigma_T^{-1}e_T \right) \right) \\ &\propto IW\left(\Sigma_T \middle| \nu+1, \left(S_{T-1}^{-1} + e_T e_T' \right) \right) \quad : \text{proposal density} \\ &\quad \times \exp\left(-\frac{1}{2}\left(\epsilon_T'\Sigma_T^{-1}\epsilon_T - e_T'\Sigma_T^{-1}e_T \right) \right) \quad : \text{MH correction} \end{aligned}$$

where we define e_T in the same as before. We draw Σ_T based on the independent Metropolis-Hastings algorithm with the inverse Wishart distribution as a proposal distribution, $\Sigma_T^* \sim IW\left(\nu+1, \left(S_{T-1}^{-1} + e_T e_T'\right)\right)$ and therefore the acceptance ratio is

$$r_{\Sigma_T} = \left\{ \frac{\exp\left(-\frac{1}{2}\left((\epsilon_T^*)'(\Sigma_T^*)^{-1}\epsilon_T^* - e_T'(\Sigma_T^*)^{-1}e_T \right) \right)}{\exp\left(-\frac{1}{2}\left((\epsilon_T^{old})'(\Sigma_T^{old})^{-1}\epsilon_T^{old} - e_T'(\Sigma_T^{old})^{-1}e_T \right) \right)}, 1 \right\}$$

where

$$\epsilon_T^* = \underbrace{Y_T - \mu - \Phi Y_{T-1}}_{=e_T} - Bf(\Sigma_T^*) = e_T - Bf(\Sigma_T^*).$$

We set $\Sigma_T^{new} = \Sigma_T^*$ with probability $\min(r_{\Sigma_T}, 1)$, $\Sigma_T^{new} = \Sigma_T^{old}$ otherwise. We consider a mixture proposal distribution with the above proposal distribution and a random walk MH type proposal distribution as in step 2.

Step 4: $(\boldsymbol{\mu}, \boldsymbol{B}, \boldsymbol{\Phi})$ First we transform our model into the following multiple regression form,

$$\widetilde{Y}_t = \widetilde{B}\widetilde{X}_t + \Sigma_t^{1/2}\epsilon_t, \quad \epsilon_t \sim N(0, I)$$

where p is the number of lags in VAR and

$$\begin{aligned}
\widetilde{Y}_t &= Y_t' \\
\widetilde{X}_t &= [1, Y_{t-1}', ..., Y_{t-p}', f(\Sigma_t)']' \\
\widetilde{B} &= [\mu, \Phi_1, ..., \Phi_p, B].
\end{aligned}$$

Then, we can re-write the equation as

$$\Sigma_t^{-1/2}\widetilde{Y}_t = \left(\widetilde{X}_t' \otimes \Sigma_t^{-1/2}\right) vec\left(\widetilde{B}\right) + \epsilon_t,$$

which is a standard multiple regression with homoscedastic errors. The conditional posterior distribution of (μ, B, Φ) is a multivariate normal distribution under the conjugate prior assumption.

Step 5: $\boldsymbol{\nu}$ The conditional posterior distribution of ν is

$$p(\nu|others) \propto \left(\prod_{t=1}^{T} \frac{|S_{t-1}^{-1}|^{\nu/2}}{2^{\nu k/2}\Gamma_k(\nu/2)} |\Sigma_t|^{-(\nu+k+1)/2} exp\left(-\frac{1}{2} tr(S_{t-1}^{-1}\Sigma_t^{-1})\right)\right) p_G(\nu)\mathbf{1}_{(k+1,M_\nu)}(\nu)$$

where $S_{t-1}^{-1} = (v-k-1)(C + A\Sigma_{t-1}A')$, $\Gamma_k(\cdot)$ is the multivariate gamma function, $p_G(\nu)$ is a prior distribution for nu, which is set to be Gamma distribution, and $\mathbf{1}_{(k+1,M_\nu)}(\nu)$ is a indicator function takes value 1 if $\nu \in (k+1, M_\nu)$ and 0 otherwise. To draw ν from this conditional posterior distribution, we employ the random-walk Metropolis-Hastings algorithm with a proposal

$$\nu^* = \nu^{old} + e_\nu, \quad e_\nu \sim N(0, \sigma_\nu^2)$$

where the scale of the proposal distribution σ_ν^2 is adaptively chosen so that the resulting acceptance rate is about 30% (Atchadé and Rosenthal, 2005).

Step 6: $\boldsymbol{C}$ The conditional posterior distribution of C is

$$\begin{aligned}
p(C|others) \propto &\left(\prod_{t=1}^{T} |S_{t-1}^{-1}|^{\nu/2} |\Sigma_t|^{-(\nu+k+1)/2} exp\left(-\frac{1}{2} tr(S_{t-1}^{-1}\Sigma_t^{-1})\right)\right) \times p_{IW}(C|df, \Psi) \\
&\times p_{IW}\left(\nu_0, V_0^{-1}\right), \quad \text{where } V_0^{-1} = (v_0 - k - 1)(I - \overline{A})^{-1}\overline{C},
\end{aligned}$$

and $S_{t-1}^{-1} = (v-k-1)(C + A\Sigma_{t-1}A')$, and p_{IW} is a density function of the inverse Wishart distribution. In this step, we reparametrize C in the following fashion,

$$C = \begin{pmatrix} d_{11} & 0 & \dots & 0 \\ c_{21} & d_{22} & \dots & 0 \\ \vdots & & \ddots & 0 \\ c_{k1} & c_{k2} & c_{k3} & \dots d_{kk} \end{pmatrix} \begin{pmatrix} d_{11} & 0 & \dots & 0 \\ c_{21} & d_{22} & \dots & 0 \\ \vdots & & \ddots & 0 \\ c_{k1} & c_{k2} & c_{k3} & \dots d_{kk} \end{pmatrix}'.$$

This transformation ensures the positive definiteness of C. To draw C from this conditional posterior distribution, we employ the random-walk Metropolis-Hastings algorithm with a proposal

$$\begin{aligned} c_{ij}^{*} &= c_{ij}^{old} + e_{c(i,j)}, \quad e_{c(i,j)} \sim N(0, \sigma_{c(i,j)}^2) \\ \log(d_{ii}^{*}) &= \log(d_{ii}^{old}) + e_{d(i,i)}, \quad e_{d(i,i)} \sim N(0, \sigma_{d(i,i)}^2) \end{aligned}$$

for $(i,j) = \{i = 1,..,k; j = 1,...,k, i \geq j\}$. The scale of the proposal distribution $\sigma_{c(i,j)}^2$ and $\sigma_{d(i,j)}^2$ are adaptively chosen so that the resulting acceptance rate is about 30% (Atchadé and Rosenthal, 2005). Note that to compute the acceptance ratio, we need a Jacobian term due to reparametrization,

$$|J| = \underbrace{2^k \prod_{i=1}^{k} d_{ii}^{k+1-i}}_{cholsky\ decomp.} \times \underbrace{\prod_{i=1}^{k} d_{ii}}_{log\ trans.}.$$

Step 7: *A* The conditional posterior distribution of A is

$$\begin{aligned} p(A|others) \propto & \left(\prod_{t=1}^{T} |S_{t-1}^{-1}|^{\nu/2} |\Sigma_t|^{-(\nu+k+1)/2} exp\left(-\frac{1}{2} tr(S_{t-1}^{-1}\Sigma_t^{-1}) \right) \right) \\ & \times p_{TN}\left(A_{11} | m_{A(1,1)}, V_{A(1,1)}, 0, \infty \right) \prod_{(i,j)\neq(1,1)} p_N\left(A_{ij}, m_{A(i,j)}, V_{A(i,j)} \right) \\ & \times p_{IW}\left(\nu_0, V_0^{-1} \right), \quad \text{where } V_0^{-1} = (v_0 - k - 1)(I - \overline{A})^{-1}\overline{C}. \end{aligned}$$

and $S_{t-1}^{-1} = (v-k-1)(C + A\Sigma_{t-1}A')$, p_{TN} is a density function of the truncated normal distribution, and p_N is a density function of the normal distribution. Note that the sign of $A_{(1,1)}$ is not identified. Hence, we place the prior distribution over $A_{(1,1)} > 0$.

To draw A from this conditional posterior distribution, we employ the element-wise

random-walk Metropolis-Hastings algorithm with a proposal,

$$A^*_{(i,j)} = A^{old}_{(i,j)} + w_{i,j}, \quad w_{i,j} \sim N\left(0, \sigma^2_{A_{(i,j)}}\right),$$

where the scale of the proposal distribution $\sigma^2_{A(i,j)}$ is adaptively chosen so that the resulting acceptance rate is about 30% (Atchadé and Rosenthal, 2005) for each (i, j).

B Prior specification

In this section, we present the prior distributions used for the application section. Our benchmark model is the CAIW(1)-in-VAR(12) model with $log(diag(\Sigma_t))$ as a linking function. Parameters in the conditional mean of the model, μ, Φ and B, are assumed to follow independent multivariate normal distributions,

$$\mu \sim N\left(0_4,\ 10^2 \cdot I_4\right), \quad vec(B) \sim N\left(0_4,\ 10^2 \cdot I_4\right), \quad vec(\Phi_1) \sim N\left(vec(I_{16}),\ 10^2 \cdot I_{16}\right)$$
$$vec(\Phi_i) \sim N\left(0_{16},\ 10^2 \cdot I_{16}\right) \quad \text{for } i = 2, ..., 12.$$

where $vec(\cdot)$ is the vectorize operator, $0_\#$ is a $\# \times 1$ vector of zeros, and $I_\#$ is a $\# \times \#$ identity matrix. There are three types of parameters in the volatility equation (A, C, and ν). The parameter A governs the dynamic properties of the volatility matrix process. Each element of A follows an independent normal distribution except the element in the far upper-left corner. The prior distribution for the $(1, 1)$-th element in the A matrix is set to be a truncated normal distribution defined on the positive real line to ensure identification.

$$A(1,1) \sim TN(0.9,\ 0.1^2, 0, \infty), \quad A(i,i) \sim N(0.9,\ 0.1^2) \quad \text{for } i = 2, 3, 4$$
$$A(i,j) \sim N(0, 0.1^2) \quad \text{for } i \neq j.$$

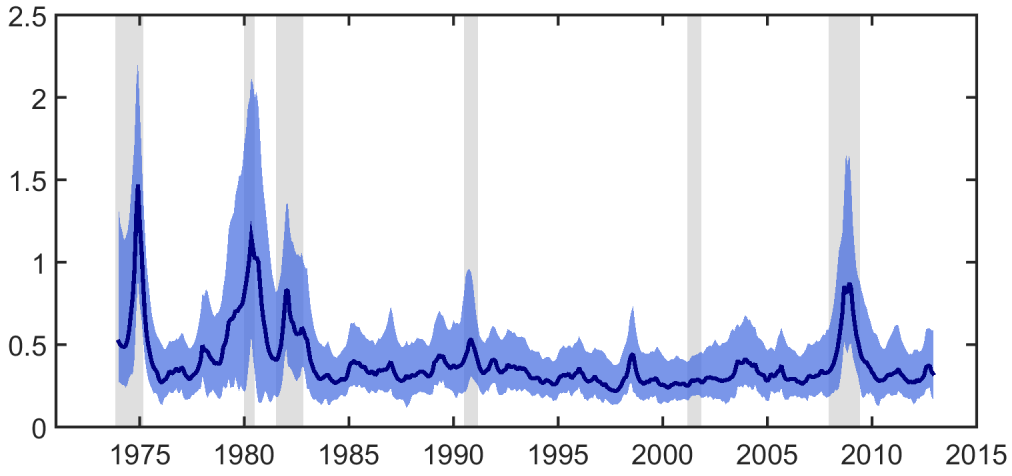
The parameter C determines the long-run mean of the volatility process. We set the prior for it as following an inverse Wishart distribution with scale matrix Ψ and degrees of freedom parameter df. We set the scale matrix to be $\Psi = diag([0.9, 0.15, 1.0, 0.3]/20)$ and the degrees of freedom parameter to bet $df = 15$. As the Wishart-type distribution is quite a popular prior in the Bayesian literature for a variance covariance matrix, we believe it to be a natural choice for C and $C \sim IW(4, I_4)$. Finally, the prior distribution for ν follows a Gamma distribution with mean 40 and standard deviation 1.

C Posterior estimates

C.1 Stochastic volatility estimates

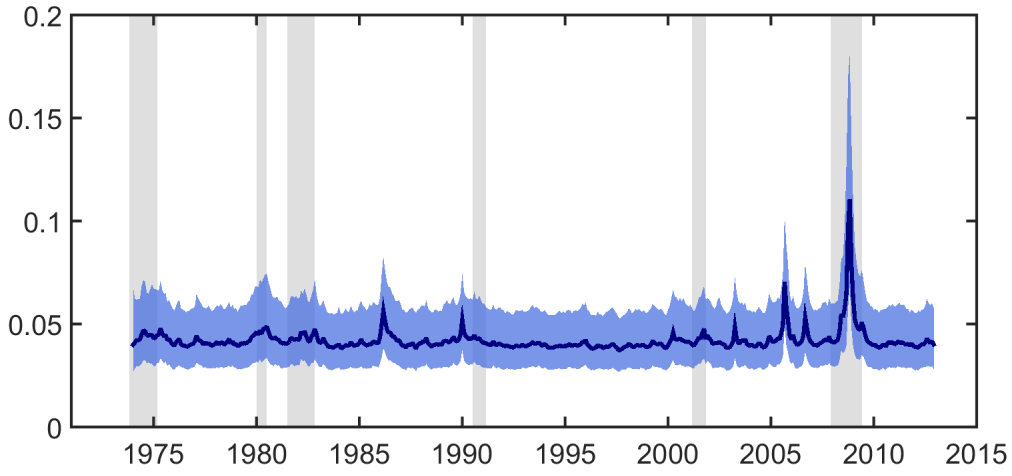
Estimated stochastic volatility series are presented in figures A-1 through A-4.

Figure A-1 Estimated Stochastic Volatility, IP



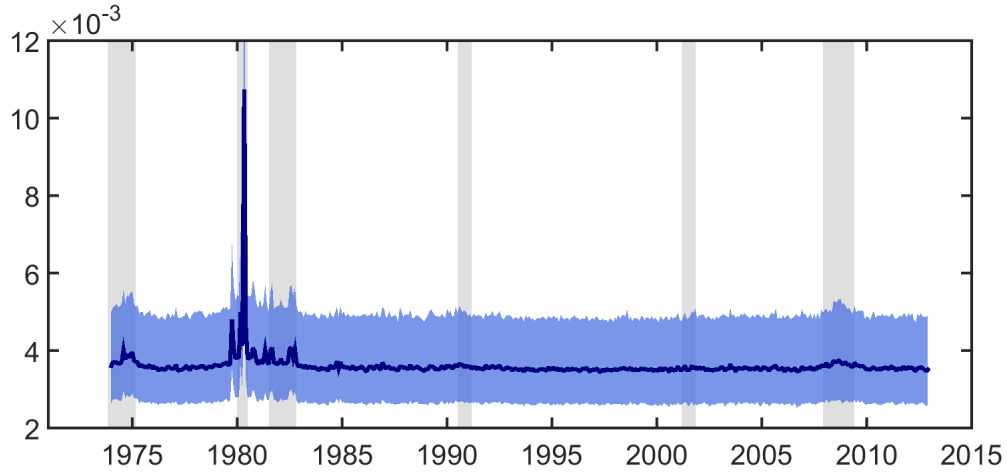
Note: Estimated stochastic volatility for IP based on the CAIW(1)-in-VAR(12) model.

Figure A-2 Estimated Stochastic Volatility, CPI



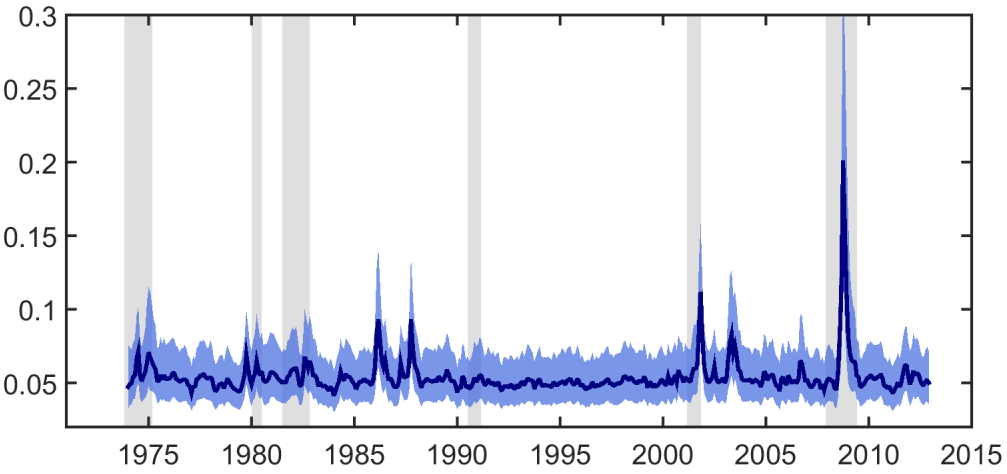
Note: Estimated stochastic volatility for CPI based on the CAIW(1)-in-VAR(12) model.

Figure A-3 Estimated Stochastic Volatility, Federal funds rate



Note: Estimated stochastic volatility for the federal funds rate based on the CAIW(1)-in-VAR(12) model.

Figure A-4 Estimated Stochastic Volatility, Excess bond premium



Note: Estimated stochastic volatility for the excess bond premium based on the CAIW(1)-in-VAR(12) model.

C.2 Details on the structural model

The dynamic equilibrium model emphasizes the mechanism highlighted in Gertler and Karadi (2011). The setup is quite similar to the baseline Gertler and Karadi (2011) model, but with three main differences: agents have Epstein-Zin utility, the government does not follow any credit policy, and price setters face Rotemberg (1982) as opposed to Calvo adjustment costs.

Please refer to Gertler and Karadi (2011) for a discussion of model details[12]. This exposition will be a general sketch of the model.

There are two types of households: workers and bankers (financial intermediaries). Households have Epstein-Zin utility over consumption and leisure. Workers maximize consumption (C_t), labor (L_t), one period real deposit holdings (B_t), and one period nominal deposit holdings (B_T^n). P_t is the price level, W_t is the real wage rate, R_t is the real return on one period risk free deposits, ir_t is the nominal risk free rate on one period deposits, Π_t are profits from firms, and T_t are transfers.

$$U_t = \max_{C_t, L_t, B_t} \left[\left(C_t^{\eta} (1 - L_t)^{1-\eta} \right)^{\frac{1-\sigma}{\theta_U}} + \beta \left(E_t U_{t+1}^{1-\sigma} \right)^{\frac{1}{\theta_U}} \right]^{\frac{\theta_U}{1-\sigma}} \tag{A.1}$$

subject to

$$C_t = W_t L_t + \Pi_t + T_t + R_t B_t - B_{t+1} + ir_{t-1} \frac{B_t^n}{P_t} - \frac{B_{t+1}^n}{P_t}$$

Financial intermediaries obtain deposits from households and use the funds raised as well as their own net worth to lend to non-financial firms. An intermediary j has the following balance sheet constraint, where Q_t is the price of a claim on non-finanical firms, $S_{j,t}$ is the quantity of claims, $N_{j,t}$ is the net worth, and $B_{j,t+1}$ is the amount of deposits:

$$Q_t S_{j,t} = N_{j,t} + B_{j,t+1} \tag{A.2}$$

Intermediary net worth has the following law of motion, where $R_{k,t+1}$ is the realized return to capital in period $t+1$:

$$N_{j,t+1} = R_{k,t+1} Q_t S_{j,t} - R_{t+1} B_{j,t+1} = \left(R_{k,t+1} - R_{t+1} \right) Q_t S_{j,t} + R_{t+1} N_{j,t} \tag{A.3}$$

Intermediary j's objective function is to maximize expected terminal wealth adjusted by the household stochastic discount factor ($\beta^i \Lambda_{t,t+i}$)

$$V_{j,t} = \max E_t \left(\sum_{\tau=1}^{\infty} (1-\theta) \theta^{\tau} \beta^{\tau} \Lambda_{t,t+\tau} \left[\left(R_{k,t+\tau} - R_{t+\tau} \right) Q_{t+\tau-1} S_{j,t+\tau-1} + R_{t+\tau} N_{j,t+\tau-1} \right] \right) \tag{A.4}$$

A banker has the following incentive compatibility constraint, motivated by a desire to divert assets, only $1 - \lambda$ of which can be recovered by the households

$$V_{j,t} \geq \lambda Q_t S_{j,t} \tag{A.5}$$

[12] The appendix of Foerster (2015) also contains a useful discussion of the derivations.

Now we discuss the non-financial side of the macroeconomy. Intermediate goods firms are competitive and produce the goods that are sold to retail firms. They issue S_t claims to capital K_{t+1}. The following arbitrage relation holds between the value of claims and the value of capital:

$$Q_t K_{t+1} = Q_t S_t \tag{A.6}$$

The production function of the intermediate goods firms is Cobb-Douglas and perturbed by a permanent TFP shock (A_t) and capital quality shock (ζ_t):

$$Y_t = (U_t \zeta_t K_t)^{\alpha} (A_t L_t)^{1-\alpha} \tag{A.7}$$

where U_t is capacity utilization.

Before selling previously purchased capital back on the competitive market, intermediate goods firms also pay a unity cost per unit to repair depreciated capital. Therefore, the realized return to capital K_{t+1} is

$$R_{k,t+1} = \frac{\left[P_{m,t+1}\alpha \frac{Y_{t+1}}{\zeta_{t+1}K_{t+1}} + Q_{t+1} - \delta(U_{t+1})\right]\zeta_{t+1}}{Q_t} \tag{A.8}$$

where $P_{m,t+1}$ is the price of intermediate goods. In addition to purchasing capital, intermediate goods firms also decide on a capital utilization rate and labor supply.

Competitive capital producing firms purchase capital from intermediate goods firms. They repair depreciated capital, build new capital, and sell it on the competitive market. In line with Gertler and Karadi (2011), we assume that adjustment costs are on investment net of depreciated capital. Therefore, capital producing firms only pay a unit cost to repair depreciated capital. Their profits are as follows:

$$prof_t = \delta(U_t)\zeta_t K_{t-1} - Q_t \zeta_t K_{t-1} + Q_t K_t - (K_t - (1-\delta(U_t))\zeta_t K_{t-1}) - S\left(\frac{I_{n,t} + I_{ss}A_t}{I_{n,t-1} + I_{ss}A_{t-1}}\right)(I_{n,t} + I_{ss}A_t) \tag{A.9}$$

We define net investment as

$$I_{n,t} = I_t - \delta(U_t)\zeta_t K_t \tag{A.10}$$

Rewriting the profits of capital producing firms in terms of net investment, the maximization problem is as follows:

$$\max_{I_{n,t}} E_t \left(\sum_{\tau=0}^{\infty} \beta^{\tau} \Lambda_{t,t+\tau} \left[(Q_\tau - 1) I_{n,\tau} - S\left(\frac{I_{n,\tau} + I_{ss}A_\tau}{I_{n,\tau-1} + I_{ss}A_{\tau-1}}\right)(I_{n,\tau} + I_{ss}A_\tau) \right] \right) \tag{A.11}$$

The function S is quadratic with respect to changes in net investment. I_{ss} is the trend-adjusted steady state level of investment. Capital good producers choose net investment levels $I_{n,\tau}$ to maximize the expected future discounted value of firm profits.

Retail firms are monopolistically competitive. They buy inputs from intermediate goods firms. The final output is a CES aggregate of each retail firm f product:

$$Y_t = \left[\int_0^1 Y_{ft}^{\frac{\epsilon-1}{\epsilon}} df\right]^{\frac{\epsilon}{\epsilon-1}} \tag{A.12}$$

Retail firms face quadratic price adjustment costs and have the objective function

$$\max E_t \sum_{\tau=0}^{\infty} \beta^\tau \Lambda_{t,t+\tau} \left(\left(\frac{p_{f,t+\tau}}{p_{t+\tau}} - P_{m,t+\tau} \right) \left(\frac{p_{f,t+\tau}}{p_{t+\tau}} \right)^{-\epsilon} y_{t+\tau} - \frac{\phi_p}{2} \left(\frac{p_{f,t+\tau}}{\Pi p_{f,t+\tau-1}} - 1 \right)^2 y_{t+\tau} \right) \tag{A.13}$$

Monetary policy follows a standard Taylor rule with interest rate smoothing that reacts to inflation and output growth deviations from steady state.

$$\frac{ir_t}{ir} = \left(\frac{ir_{t-1}}{ir} \right)^{\rho_R} \left(\left(\frac{\Pi_t}{\Pi} \right)^{\rho_\pi} \left(\frac{\Delta \log Y_t}{\Lambda_A} \right)^{\rho_Y} \right)^{1-\rho_R} \tag{A.14}$$

The Euler equation for nominal bonds holds:

$$\beta E_t \left(\Lambda_{t,t+1} \frac{ir_t}{\Pi_{t+1}} \right) = 1 \tag{A.15}$$

The government fiscal policy is Ricardian. Goods market clearing implies, where G is a fixed, exogenous level of government spending:

$$Y_t = C_t + I_t + \frac{\phi_p}{2} \left(\frac{\Pi_t}{\Pi} - 1 \right)^2 Y_t + S \left(\frac{I_{n,t} + I_{ss} A_t}{I_{n,t-1} + I_{ss} A_{t-1}} \right) (I_{n,t} + I_{ss} A_t) + G \tag{A.16}$$

The capital accumulation equation is:

$$K_{t+1} = (1 - \delta(U_t)) \zeta_t K_t + I_t \tag{A.17}$$

Depreciation $\delta(U_t)$ is a function of the amount of utilization

$$\delta(U_t) = \delta + \gamma_1 (U_t - 1) + \gamma_2 (U_t - 1)^2 \tag{A.18}$$

The two exogenous shocks and their stochastic volatilities follow autoregressive processes:

$$\begin{aligned}
&\Delta \log A_t = \rho_A \Delta \log A_{t-1} + \epsilon_{A,t}, \epsilon_{A,t} \sim N(0, h_A^2) \\
&h_{A,t} = (1-\rho_{h,A})\sigma_A + \rho_{h,A} h_{A,t-1} + \epsilon_{h_A,t}, \epsilon_{h_A,t} \sim N(0, \sigma_{h,A}^2) \\
&\log \zeta_t = \rho_\zeta \log \zeta_{t-1} + \epsilon_{\zeta,t}, \epsilon_{\zeta,t} \sim N(0, h_\zeta^2) \\
&\log h_{\zeta,t} = (1-\rho_{h,\zeta})\sigma_\zeta + \rho_{h,\zeta} \log h_{\zeta,t-1} + \epsilon_{\zeta,t}, \epsilon_{\zeta,t} \sim N(0, \sigma_{h,\zeta}^2)
\end{aligned} \tag{A.19}$$

Table A-1 Parameter values of the dynamic equilibrium model considered in the main text

Parameter	Value	Parameter	Value
α	0.33	ρ_A	0.2
β	0.994	σ_A	0.007
Λ_A	0.004	ρ_ζ	0.66
Π	0.0092	σ_ζ	0.01
ϵ	6	$\rho_{h,A}$	0.5
δ	0.025	$\sigma_{h,A}$	0.5
η	0.32	$\rho_{h,\zeta}$	0.5
σ	10	$\sigma_{h,\zeta}$	0.5
ψ	36	G	$0.19Y_{ss}$
γ_2	0.01	$R_{k,ss} - R_{ss}$	0.01/4
S''	3		
ϕ_p	160		
ρ_R	0.75		
ρ_π	1.5		
ρ_y	0.5		
θ	0.972		
λ	0.381		

C.3 Comparison of empirical results to proxy VAR

To compare our results with the current literature, we also consider two sets of vector autoregressions using uncertainty proxies. The first uses the uncertainty factor proposed by Jurado et al. (2015). This uncertainty factor comes from the cross-sectional average of the time-varying volatilities from the unpredictable components of a large set of macroeconomic variables. It has been put forth as a measure of aggregate macroeconomic uncertainty. The second is the VXO, which is a measure of the option-implied expected volatility of the S&P100 for the following month. This measure of stock market volatility has been quite popular in the literature as a proxy for macroeconomic uncertainty.

For the results with the uncertainty proxy of Jurado et al. (2015), we estimate the data from $1973M1 - 2011M12$ on the same set of variables as our empirical application with 12 lags in the VAR. The VXO data only begins in $1986M1$, so we begin the estimation at that point when using the VXO as the volatility proxy[13]. We impose flat priors on the VAR. We use a Cholesky decomposition to identify the uncertainty shock, with the variable ordering of the volatility proxy, excess bond premium, industrial production, consumer price index, and the federal funds rate. This ordering allows the excess bond premium to respond to uncertainty shocks contemporaneously. We consider a Cholesky identification because it is by far the most popular in the empirical literature (several examples include Bloom (2009), Baker et al. (2013), Fernandez-Villaverde et al. (2015), Basu and Bundick (2015), and Jurado et al. (2015))[14].

Figure A-5 shows the effects of the identified uncertainty shock on the uncertainty proxies. This gives a sense of the persistence of uncertainty implied by the different proxies. The left panel shows the results for the VAR using the macro uncertainty factor whereas the right panel shows the results for the VAR using the VXO. While uncertainty implied by the Jurado et al. (2015) factor persists for 20 months, uncertainty implied the VXO persists for only 8 months. Focusing on the increase in IP volatility from our identified uncertainty shock, we find that volatility increases for 12 months, which is closer to the VXO results than the Jurado et al. (2015) results.

Figure A-6 shows the impact of a 1 standard deviation uncertainty shock on the macroeconomy using the macro uncertainty factor compared to the posterior median results from the $\mathcal{A}_{uf}$ identification. The uncertainty shock identified using the Jurado et al. (2015) factor

[13] As a robustness check, we also rerun the model with the Jurado et al. (2015) proxy beginning in $1986M1$. The qualitative results do not change.

[14] Note that we also tried to implement a similar sign restrictions identification strategy as in our baseline results, namely imposing an increase in the uncertainty proxy on impact and an increase in the excess bond premium for 3 months, but we did not get significant results for either proxy.

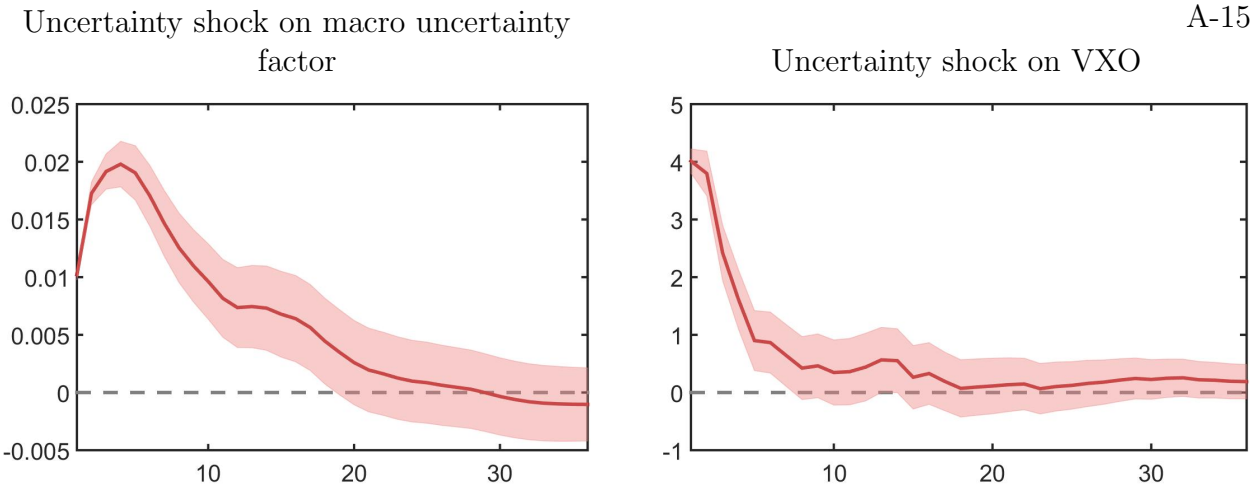


Figure A-5 Effect of 1 standard deviation positive uncertainty shock on uncertainty proxies with Cholesky identification. The left panel shows the results for the VAR using the macro uncertainty factor whereas the right panel shows the results for the VAR using the VXO. Dark lines give posterior median results. Bands indicate 80% posterior intervals. Time period is in months.

leads to a large, protracted decline in industrial production. Even 3 years after the shock, industrial production is still below its original trend. The decline in industrial production is also much steeper, bottoming out at around -0.7% as opposed to -0.15% with our results. On impact, both inflation and the federal funds rate increase when using the uncertainty proxy. With our identification strategy, there is little evidence of a movement in inflation and the federal funds rate. The excess bond premium increases in the proxy VAR, consistent with the interpretation that the identified uncertainty shock is transmitted through the financial sector. The movement in the excess bond premium is around double in magnitude when compared to our results. It persists for 10 months.

Figure A-7 compares the results from using the VXO to proxy for uncertainty and our results. A VXO-implied uncertainty shock actually leads to a transitory increase in industrial production, counterfactual to much of the economic intuition regarding the real effects of uncertainty shocks. Unlike the results from using the Jurado et al. (2015) uncertainty factor and our results, inflation and the federal funds rate declines following a VXO uncertainty shock. The excess bond premium increases for around 4 months following the uncertainty shock.

These results suggest two important conclusions[15]. First, uncertainty proxies generally

[15]The conclusions are subject to one important caveat, which is that the proxy VAR approaches allow the uncertainty proxy to respond to other macro shocks. As we discussed before, our econometric model does allow for this channel.

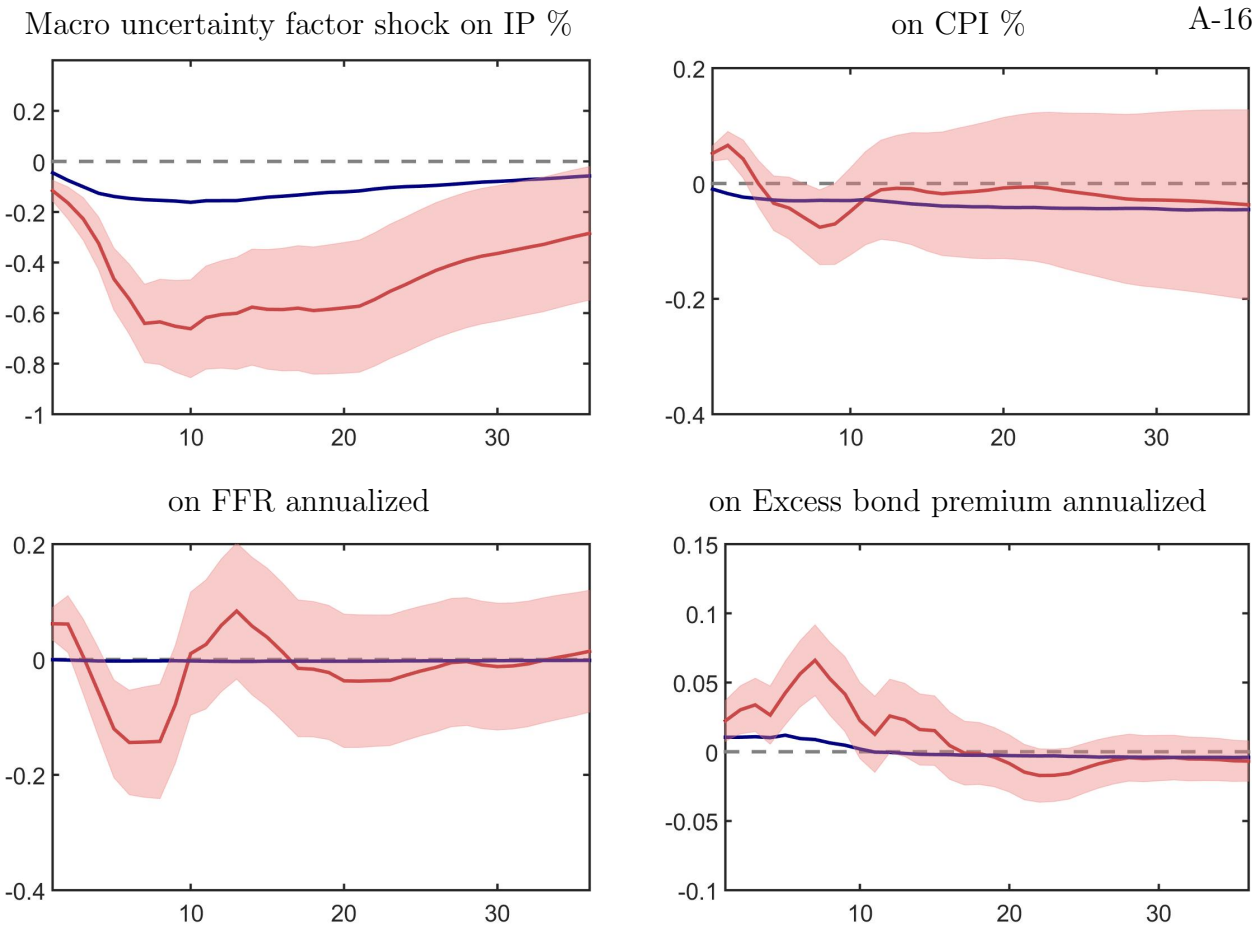


Figure A-6 Effect of 1 standard deviation positive shock to the macro uncertainty factor with Cholesky identification. Dark red lines give posterior median results. Bands indicate 80% posterior intervals. Dark blue lines give the posterior median results from our identification with Assumption $\mathcal{A}_{uf}$ imposed. Time period is in months.

give different results on the real effects of uncertainty shocks relative to the approach presented in this paper. Second, even amongst themselves, different uncertainty proxies can give conflicting results. This is most likely because different proxies measure different types of uncertainty fluctuations (financial uncertainty, political uncertainty, or a mixture of these two). This further highlights the importance of having a joint econometric framework in which the real effects of uncertainty shocks can be measured and identified internally.

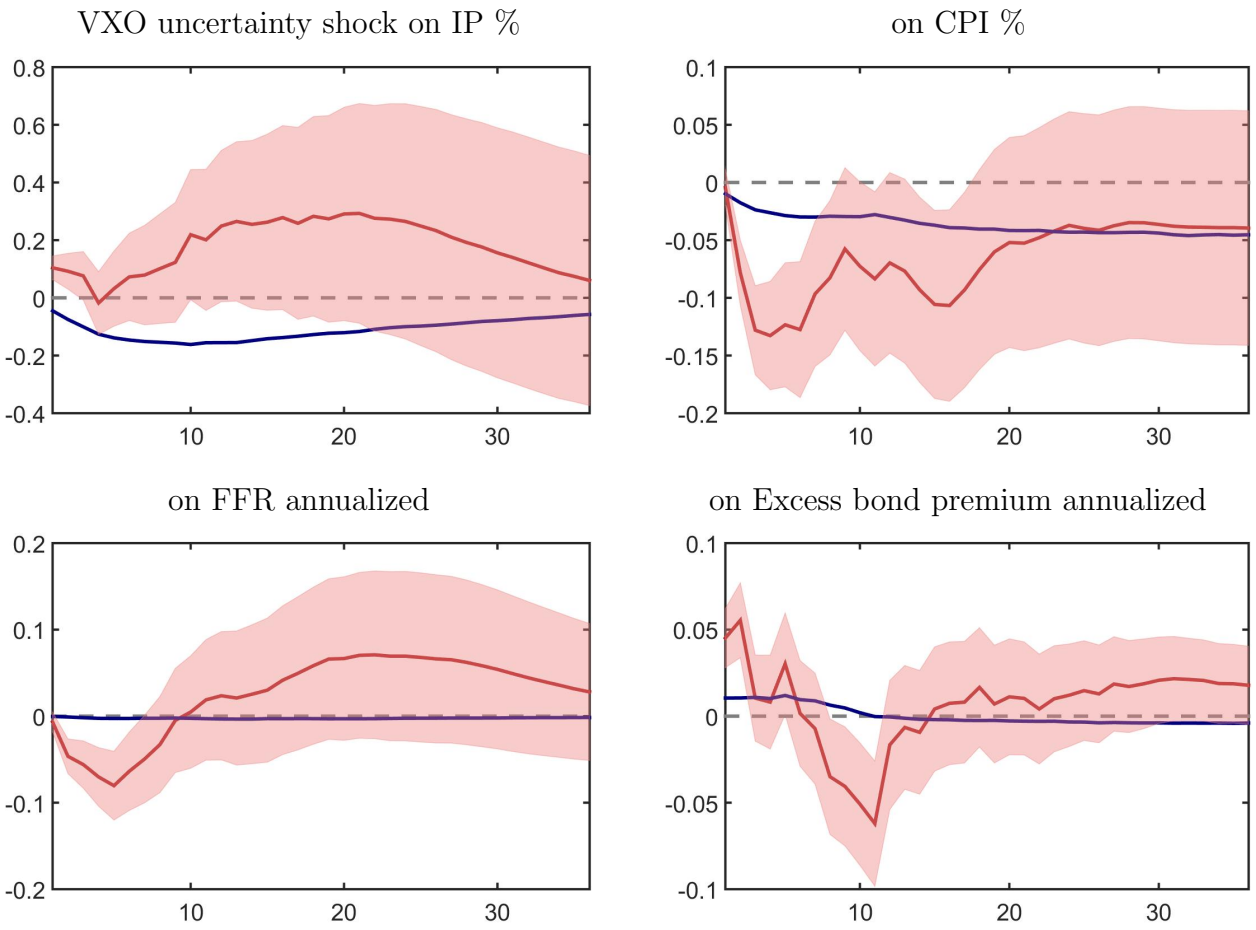


Figure A-7 Effect of 1 standard deviation positive financial uncertainty shock with Cholesky identification. Dark red lines give posterior median results. Bands indicate 80% posterior intervals. Dark blue lines give the posterior median results from our identification with Assumption $\mathcal{A}_{uf}$ imposed. Time period is in months.